DEVELOPMENT OF A CO_2-H_2O SOLID OXIDE ELECTROLYTE ELECTROLYSIS SYSTEM

by

J. Weissbart and W. H. Smart

T H I R D A N N U A L R E P O R T

March 1970

NATIONAL AERONAUTICS AND SPACE ADMINISTRATION
AMES RESEARCH CENTER
Moffett Field, California 94035

Prepared Under Contract NAS2-4843

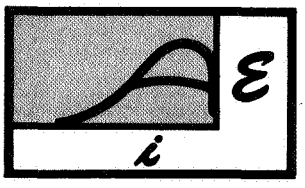

APPLIED ELECTROCHEMISTRY, INC.
735 N. PASTORIA AVE. / SUNNYVALE, CALIFORNIA 94086 / (408) 732-7880

FOREWORD

The research and development work reported here was performed at Applied Electrochemistry Incorporated, Mountain View, California, from April 1 to December 31, 1970, under Contract NAS2-4843. The work was carried out by Dr. J. Weissbart, Dr. W. H. Smart, who were the principal investigators, Mr. C. M. McCullough, Mr. B. O. Reese, Mr. S. A. Ring, Mrs. Maria Roja, and Mr. D. R. Watson. The project was under the overall direction of Dr. Weissbart. The technical monitor was Dr. T. Wydeven, Environmental Control Research Branch, NASA Ames Research Center, Moffett Field, California.

Distribution of this report is provided in the interest of information exchange. Responsibility for the contents resides in the authors and organization that prepared it.

ABSTRACT

This report describes the advances made in the development of CO_2-H_2O electrolyzer modules for the generation of oxygen for life-support systems during the concluding nine-month period of this contract. Significant improvements were made with respect to 1) ease of fabrication, 2) duration of operation with production of breathable oxygen, and 3) increase in CO_2 conversion per pass to CO for better utilization of the CO in the disproportionation reactor. Improvements were incorporated stepwise in eight electrolyzer modules which were constructed and operated with an output of breathable oxygen of >99% purity, and CO_2 conversion per pass averaging 50 percent. The modules ranged in number of cells from two to sixteen, total electrode area of 40 to 320 cm^2, total output of oxygen at 100% faradaic efficiency from 4 to 32 amperes, and CO_2 content in the oxygen of <1 percent. The operating period ranged from 11 to 101 days. A 12-cell, 24-A unit operated for 101 days at an average cell voltage of 1.8 volt. The largest unit of 16 cells continues to operate at 32 A and an average voltage per cell of 1.6 volt after logging 82 days of maintenance-free operation.

The basic building block of these electrolyzer modules remained 7 to 8 mole% scandia-stabilized zirconia disk electrolytes of 20 cm^2 area constructed in the form of two-cell drums. New gas port entry nozzles were incorporated into the drums. The assembly of drums to the gas manifold tubes was made by torch brazing. Improved electrode-grid configurations consisted of an overlay of fine Pt mesh reinforced with high electrical conductivity Au alloy wire. These and other improvements in hot pressing and fabrication of gas-tight high-temperature ceramic seals now allows construction of modules for one-man capacity units producing breathable oxygen (>99%) and having an operating life of >3 months.

CONTENTS

ILLUSTRATIONS

TABLES

Section 1

INTRODUCTION

For extended duration space flights, O_2 generation/CO_2 control is required as part of a regenerative integrated environmental control and life-support system. The Hamilton Standard Division of United Aircraft Corporation has recently evaluated and selected life-support systems presently under development for a 500-day non-resupply mission for the 1976-1980 time period. The most promising route chosen for oxygen recovery from CO_2 was electrolysis using solid oxide electrolytes and CO disproportionation using replaceable cartridges (Ref. 9).

Work on contract NAS2-4843 previously presented in the First and Second Annual Reports (Refs. 1 and 2) has taken the CO_2-H_2O oxygen generation system based on solid oxide electrolytes from the 1/100-man (one ampere) to the one-man (127 amperes) level. The utilization of hot pressing of ceramics, diamond machining, electroplating of ceramics, fabrication of gas-tight high-temperature ceramic seals, and other technologies was required to bring the development of this system to that stage. A 127-A capacity CO_2-H_2O electrolyzer/CO disproportionation reactor system was constructed and operated beyond 250 hours (Ref. 2).

The nine-month effort described in this Third Annual Report concludes the development work on contract NAS2-4843 and bridges the gap between the two-year effort on contract NAS2-4843 and the next stage—the development of hardware for an integrated one-man oxygen generation system consisting of a bank of CO_2-H_2O electrolyzers, CO disproportionator, pump and closed recycle loop, with instrumented control panel.

The purpose of this nine-month effort was the continuation and further improvement of the design, components, and fabrication procedures of modules of the size required for a one-man unit and the obtaining of further operational and long-term reliability data for such units. This report describes the further production of stabilized zirconia compacts by hot pressing, the improvement and standardization of fabrication procedures for drums and modules, and

the work leading to the development of better electrodes and grids. The assembly and testing of eight electrolyzer modules is described. The modules contain improved ceramic-to-ceramic and ceramic-to-metal seals, improved electrodes and grids, and improved construction and assembly procedures. Based on these results, electrolyzer modules that produce breathable oxygen for at least three months on continuous operation can now be made reliably.

Section 2

HOT PRESSING

2.1 GENERAL

Forty compacts of rare earth oxide-stabilized zirconia were hot pressed this year according to the procedure described in the First and Second Annual Reports (Refs. 1 and 2). The powder compositions and hot-pressing parameters employed and the densities obtained are given in Tables 2-1, 2-2, and 2-3. An evaluation figure for the maximum relative porosity of the sliced and air-fired disks obtained from the various pressings is given in the final column. A figure of one indicates a low porosity, just enough to be significantly detectable on the vacuum leak rate test employed. A figure of approximately ten on this scale indicates a porosity high enough that a detectable leak rate of CO/CO_2 into the oxygen might be obtained if the disk were to be fabricated into an electrolyzer component. The values listed are for the most porous disk from each pressing. Due to the spatial variation of density within a given compact, Most of the disks cut from it will have porosity figures much lower than the maximum, with several having figures less than unity even when the most porous disks exceed a value of ten. All of the scandia used this year in the preparation of the powders was obtained from three packages (labeled RC3, 4, and 5 in the tables) of a single lot produced by Research Chemicals Division of Nuclear Corp. of America. The zirconium content was obtained from several different lots of oxychloride made by TAM Division of National Lead Company (and listed in the tables as TAM 11, 15/2, and 19).

2.2 Sc_2O_3 STABILIZED ELECTROLYTES

Thirteen additional compacts were prepared from powder of composition $(ZrO_2)_{0.93}(Sc_2O_3)_{0.07}$ in a continuation of the slightly lower Sc_2O_3 content series started during the previous report year (Ref. 2, Table 5-2). No disk sliced from the 22 pressings of this composition (including the nine from the previous year) had a porosity figure higher than two, and most were less than one, when made from powder prepared by our standard technique.

Most of the electrolyte material prepared during the previous two years has employed the composition $(ZrO_2)_{0.92}(Sc_2O_3)_{0.08}$.

Table 2-1

HOT PRESSINGS - $(ZrO_2)_{0.93}(Sc_2O_3)_{0.07}$ POWDER

Pressing	Powder	Source Materials	Pressure (psi)	Temp. (°C)	DENSITY		Maximum Relative Porosity
					Sp. Gr.	% of Theoretical	
G-119	B-84	RC3 TAM 15/2	3650	1560	5.66	97	<1
G-120	B-85	RC4 TAM 15/2	3620	1560	5.62	96	1
G-121	B-84, 85	RC4 TAM 15/2	3710	1560	5.64	96	2
G-122	B-86	RC4 TAM 15/2	3630	1560	5.68	97	1
G-123	B-87	RC4 TAM 15/2	3640	1570	5.64	96	1
G-125	B-86, 87	RC4 TAM 15/2	3660	1565	5.63	96	<1
G-152	B-106	RC5 TAM 19	3830	1565	5.83	99.5	<1
G-154*	B-108	RC5 TAM 19	3670	1575	5.76	98.5	<1
G-155*	B-109	RC5 TAM 19	3670	1575	5.73	98	-
G-156*	B-110**	RC5 TAM 19	3470	1575	5.78	98.8	1
G-159*	B-111**	RC5 TAM 19	3760	1535	5.77	98.7	6
G-160*	B-106, 108, 109	RC3 & 5 TAM 19	3520	1530	5.78	98.8	-
G-162*	B-109, 110, 111	RC5 TAM 19	3520	1550	5.77	98.7	<2

* Die charge increased to 432 g

** Non-standard powder preparation

Table 2-2

HOT PRESSINGS - $(ZrO_2)_{0.92}(Sc_2O_3)_{0.08}$ POWDER

Pressing	Powder	Source Materials	Pressure (psi)	Temp. (°C)	DENSITY		Maximum Relative Porosity
					Sp. Gr.	% of Theoretical	
G-130	B-92	RC4 TAM 15/2	4040	1565	5.57	95.5	13
G-131	B-93	RC4 TAM 15/2	4070	1565	5.56	95.5	4
G-132	B-94	RC4 TAM 19	4150	1565	5.66	97	<1
G-133	B-92 & 93	RC4 TAM 15/2	4120	1570	5.60	96	<1
G-134	B-95	RC4 TAM 19	4120	1570	5.66	97	<1
G-135	B-94 & 95	RC4 TAM 19	4170	1570	5.65	97	<1
G-136	B-96	RC4 TAM 19	4040	1550	5.65	97	<1
G-137	B-97	RC4 TAM 19	3830	1550	5.65	97	<1
G-138	B-96 & 97	RC4 TAM 19	3710	1555	5.60	96	<1
G-139	*	*	4040	1555	5.49	94	3
G-144	B-101	RC4 TAM 19	3840	1560	5.66	97	<1
G-145	B-102	RC4 TAM 19	3860	1565	5.64	97	<1
G-147	B-101 & 102	RC4 TAM 19	3870	1555	5.66	97	<1
G-148	B-103	RC4 TAM 19	3760	1555	5.63	97	<1
G-150	B-105	RC4 TAM 19	3810	1565	5.76	98	<1
G-153	B-103 & 105	RC4 TAM 19	3810	1570	5.70	98	<1
G-163**	B-114	RC5 TAM 19	3430	1555	5.67	97	2

* Mixed source lots including TAM 15 material

** Die charge increased to 432 g

Table 2-3

HOT PRESSINGS - SCANDIA- AND/OR YTTRIA-STABILIZED ZIRCONIA

Pressing	Powder	Source Materials	Pressure (psi)	Temp. (°C)	DENSITY		Maximum Relative Porosity
					Sp. Gr.	% of Theoretical	
$(ZrO_2)_{0.94}(Sc_2O_3)_{0.03}(Y_2O_3)_{0.03}$							
G-127	B-90	RC4 TAM 15/2	3930	1565	5.78	97	6
G-142	B-99	RC4 TAM 19	3850	1555	5.89	99	<1
G-143	B-90 & 99	RC4 TAM 19 & 15/2	3860	1555	5.85	98	<1
$(ZrO_2)_{0.93}(Sc_2O_3)_{0.04}(Y_2O_3)_{0.03}$							
G-124	B-88	RC4 TAM 15/2	3650	1570	5.63	95	8
G-126	B-89	RC4 TAM 15/2	3940	1565	5.66	96	1
G-128	B-91	RC4 TAM 15/2	4000	1570	5.63	95	5
G-129	B-88 & 89	RC4 TAM 15/2	4060	1565	5.70	97	3
G-140	B-98	RC4 TAM 19	3890	1555	5.75	97	<1
G-141	B-91 & 98	RC4 TAM 19 & 15/2	3860	1555	5.72	97	2
$(ZrO_2)_{0.91}(Y_2O_3)_{0.09}$							
G-151	B-28	- TAM 11	3810	1565*	5.67	95.5	-

* See text for special temperature program

At this Sc_2O_3 content, the overall density achieved for the hot-pressed compacts tends to be more variable (than at the seven mole percent Sc_2O_3 stabilization level) with the occasional production of sliced disks with an unacceptably high porosity. For the seventeen compacts of this composition made this year, the first two continue in this trend; however, the bulk of the recent $(ZrO_2)_{0.92}(Sc_2O_3)_{0.08}$ material is high density-low porosity.

With the completion of three years of hot pressing scandia-stabilized zirconia, some of the less obvious factors controlling the quality of the product have been discerned. The porosity of the disks sliced from a given hot-pressed compact of seven or eight mole percent scandia-stabilized zirconia is a sensitive function of the average density of the compact. The change from some porous to all non-porous disks (defined operationally for our purposes) takes place in the range 95 to 96% of theoretical density. The density of the compacts depends upon the hot-pressing conditions and the level of scandia stabilization. At the seven mole percent level it has always been possible to make high density compacts (yielding all low porosity disks) within the operational limits of the hot press. This has not always been the case at the eight mole percent level, which requires higher ram pressures to achieve equivalent density. The ram pressure requirement, to obtain a given density for a given composition, appears to correlate with the manufacturer's lot number of the TAM zirconium oxychloride used to prepare the powder (see Table 2-4). Samples from all lots of TAM, obtained during the course of this contract, were subjected to comparative emission spectographic analysis. The amounts of detectable impurities appear fairly uniform among the lots. If only the elements Si, Fe, Al, and Ti are considered (on the basis that the remainder can all be used in the formation of stabilized zirconia), the two packages from lot no. 15 may be considered as slightly "purer" than the others.

A variation in the preparation procedure was made for powder batches B-110 and B-111 (see Table 2-1). When the TAM zirconium oxychloride is dissolved, there remains a dark, gelatinous, insoluble residue. Ordinarily this residue is incorporated into the subsequent powder. For these two batches, the residue was removed by filtration. One can only speculate, at this time, as to whether the higher than usual porosity observed in compact G-159 was due to the possible removal of desirable impurities from the powder.

Table 2-4

ANALYSIS OF TAM ZIRCONIUM OXYCHLORIDE

Impurities	Lot. No. 10	Lot No. 11	Lot No. 15/1*	Lot No. 15/2*	Lot No. 19
Si	0.04%	0.05%	0.01%	0.01%	0.03%
Fe	.2	.1	.05	.08	.15
Al	.1	.05	.04	.04	.05
Mg	.01	.02	.008	.01	.004
Hf	2.5	2.5	2.	2.	2.
Ti	.025	.025	.015	.008	.03
Ca	.01	.01	<.01	<.01	<.01
Y	.06	.04	.08	.1	.06
Sc	.007	.005	.007	.007	.007
Ram Pressure Requirement	Lower**	Lower	Higher	Higher	Lower

* Manufacturer's lot no. 15 was obtained twice

** Only used for two ZrO_2-Sc_2O_3 pressings; probably "Lower"

The data in Tables 2-1 and 2-2 show that very low porosity disks can be made at both seven and eight mole percent scandia with the use of TAM lot no. 19. At these very high densities, the compacts are more difficult to slice. It has been found necessary to reduce the rate of saw advance to avoid mechanical damage to the disks. Compact G-152, pressed to almost full theoretical density, could not be sliced using our former procedure. With reduction in ram pressure (to obtain compacts with average densities in the range 97 to 98% of theoretical) a slight increase in powder charge (from the formerly used 400 g to 432 g) and careful attention to slicing procedure, it is possible to obtain six good slices from a high density compact.

2.3 OTHER RARE EARTH OXIDE STABILIZED ELECTROLYTES

Our work of the previous two years has shown that use of Y_2O_3 and/or Yb_2O_3 as the stabilization agent for zirconia, hot pressed by our technique, leads to the production of thermal shock sensitive disks, presumably due to unrelieved strain incurred during the pressing operation. We have further shown that reduction of the concentration of Y_2O_3 and/or Yb_2O_3 greatly reduces the thermal shock sensitivity. To determine whether low level stabilized zirconia might be suitable for use as electrolyte material, a disk from pressing G-92 (Ref. 2, Table 5-3) of composition $(ZrO_2)_{0.96}(Yb_2O_3)_{0.04}$ was fitted with electrodes and its ionic conductivity measured as described in Ref. 1, Section 5. The conductivity of the $(ZrO_2)_{0.96}(Yb_2O_3)_{0.04}$ disk was found to be one third of the value obtained for the highly conducting $(ZrO_2)_{0.92}(Sc_2O_3)_{0.08}$ disks in the temperature range of interest (800-900°C).

The thermal shock resistance of hot-pressed ZrO_2 stabilized at the four mole percent level with Y_2O_3 or Yb_2O_3 is still not quite as good as that for ZrO_2 stabilized with seven or eight mole percent Sc_2O_3. It appeared logical to propose that ZrO_2 stabilized with a mixture of Sc_2O_3 plus Y_2O_3 and/or Yb_2O_3 should be more resistant to thermal shock than with low Y_2O_3 and/or Yb_2O_3 alone. Such has been found to be the case. Nine compacts of ZrO_2 stabilized with Sc_2O_3 plus Y_2O_3 have been pressed, sliced, and air fired (see Table 2-3). Only two disks from these compacts have failed the standard thermal shock test. The maximum relative porosity figures for these disks are higher than might be expected. The total stabilization level does not exceed seven mole percent, where, in the

case of stabilization by Sc_2O_3 alone, low porosity material is produced, even with TAM lot no. 15 as source material. The ionic conductivity for oxygen transport for the mixed stabilizer material is lower than expected, being about the same as that measured for the $(ZrO_2)_{0.96}(Yb_2O_3)_{0.04}$ composition disk discussed above.

One hot pressing (G-151) was made using powder prepared during the first year of this contract (Ref. 1) stabilized at the nine mole percent level with yttria only. All previous hot pressings of this composition yielded electrolyte material that was too sensitive to thermal shock to be useful. In this case, the temperature program of the hot-pressing schedule was modified to include a one-hour hold at 1200°C, on the hypothesis that holding at a temperature where the bulk of the densification takes place might lead to a reduction in strain. After removal from the hot press, the compact split in half on reheating to approximately 150°C.

Section 3

IMPROVEMENT AND STANDARDIZATION OF FABRICATION PROCEDURES

3.1 CERAMIC MACHINING

3.1.1 Drum Components

The "drum" configuration of electrolyzer module sub-units has been described in Ref. 2. Most of the drum bodies (and all those used in electrolyzers) have been fabricated from slices cut from tubes or crucibles of zirconia partially stabilized with calcia. These tubes and crucibles, obtained from an outside vendor (Zirconium Corporation of America), vary considerably in diameter, wall thickness and roundness for any given nominal size. To produce a drum body with the edge seal configuration (Fig. 3-1), it is necessary to machine a step on the interior diameter of each end of the slice, to accommodate the electrolyte disk and the braze fillet. The steps in the early edge seal drum bodies were successfully machined with the use of a special coring tool, shown in Fig. 3-2. Although excellent seals were obtained in bodies with core-drilled steps, only a few of the tubes and crucibles supplied by the vendor were uniform enough to be machined by this method.

A greater flexibility in ceramic machining was attained by modifying a standard metal working lathe to take a grinding motor in place of the normal tool holder (see Fig. 3-3). With the ceramic part held in the jaws of the lathe and a diamond grinding wheel in the chuck of the tool motor, a number of precise machining operations can be accomplished in addition to formation of drum steps to any desired inside diameter. Most of the vendor-supplied stock can now be used to prepare drum bodies.

The standard procedure for the preparation of edge seal drum assemblies entails slicing the tube stock on a diamond-edged cut-off saw and grinding the cut ends flat and parallel on a diamond polishing wheel. The four holes, for gas port tubes and electrical leads, are drilled with diamond impregnated bits in oscillating high-speed drill presses. The outside of the drum body is finished round on the lathe grinding machine. The steps are cut in 0.100 inch (0.25 cm) from each end and then the inside is finished concentric with the outside. A

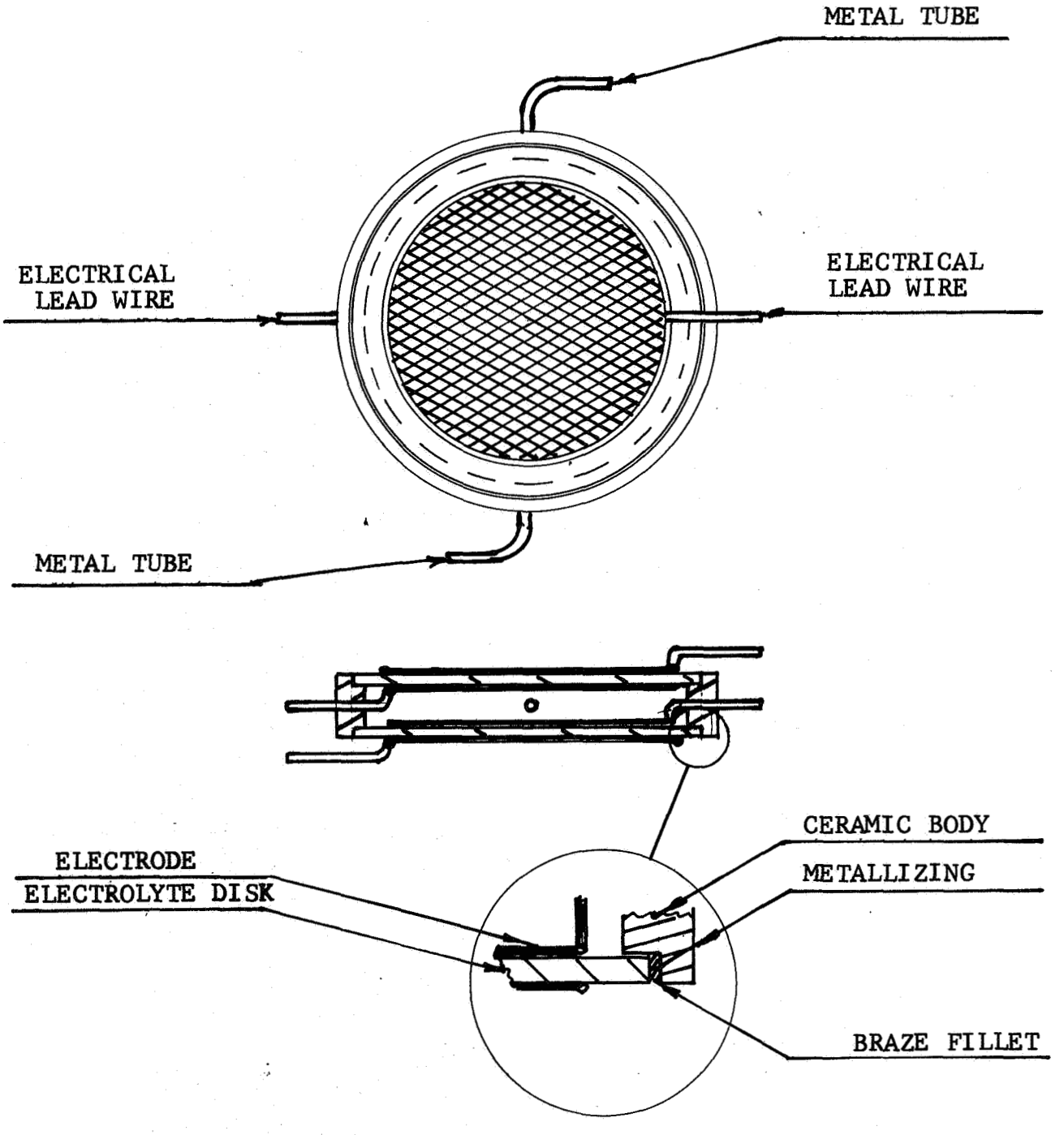

Fig. 3-1 Drum with Edge Seals

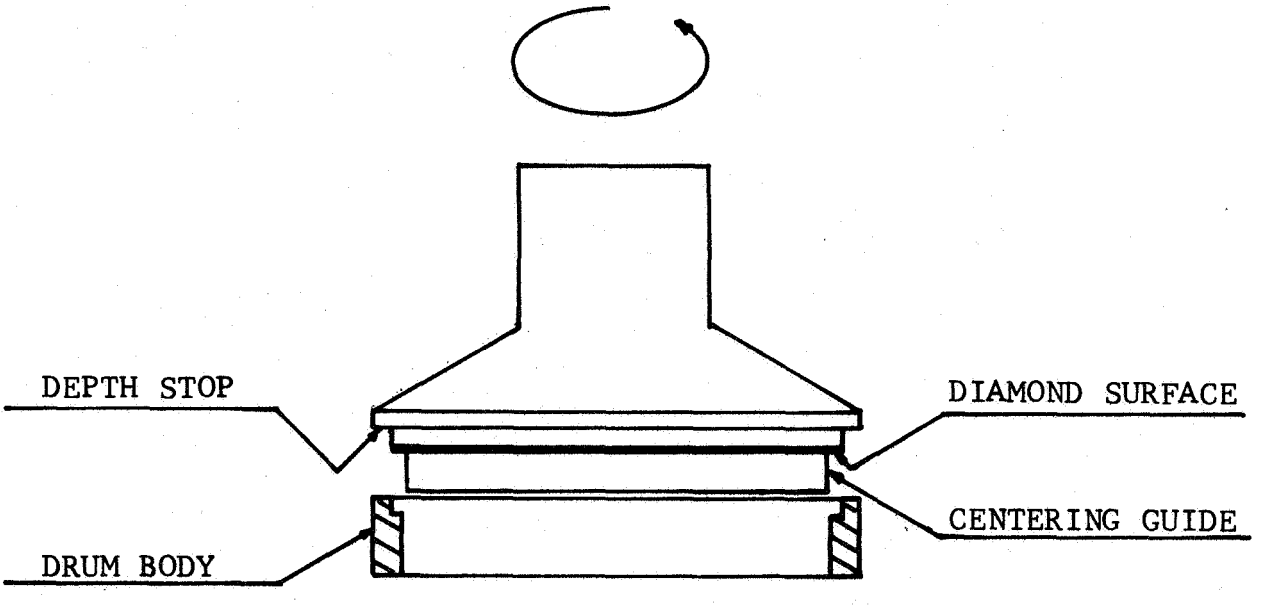

Fig. 3-2 Coring Tool

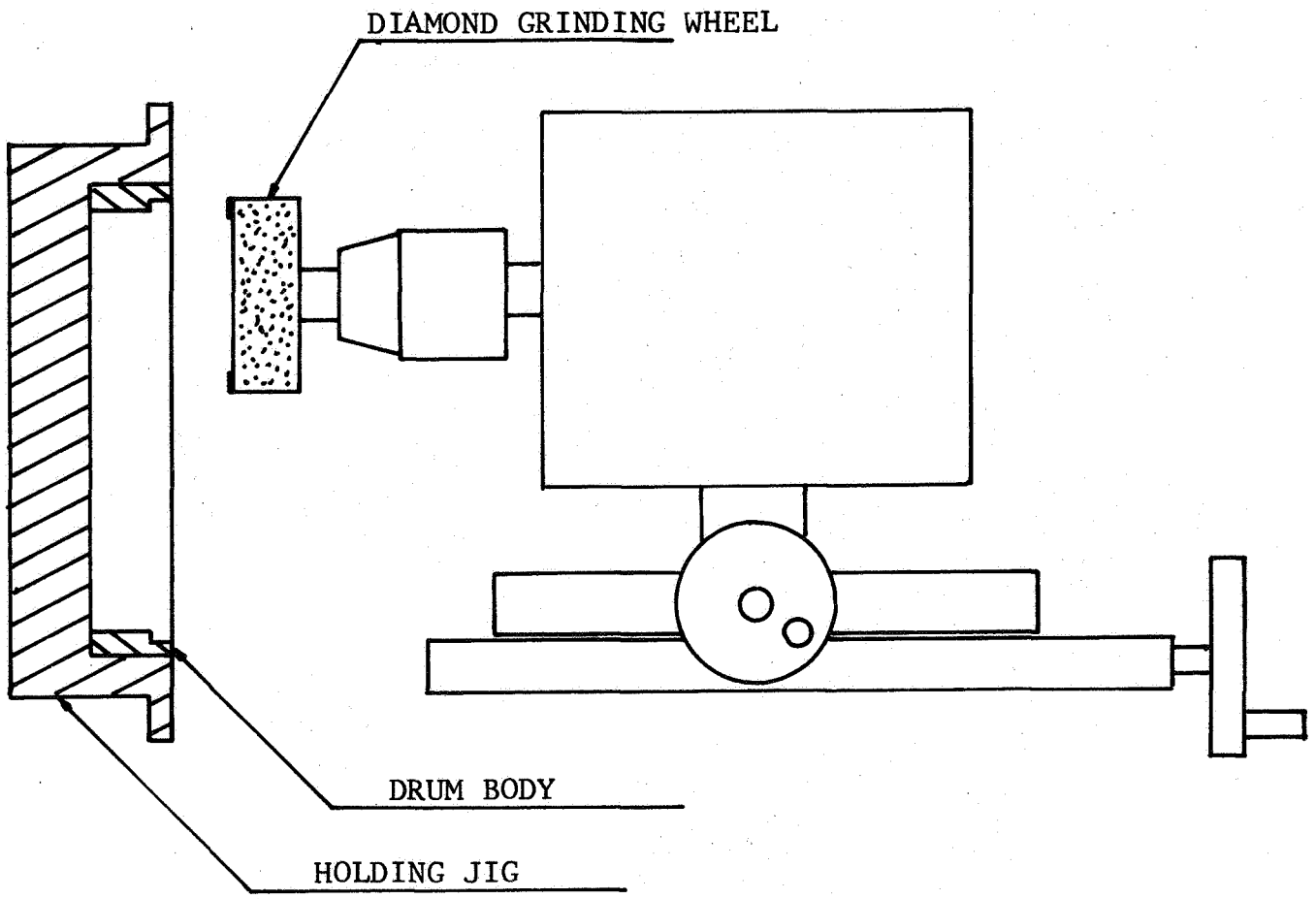

Fig. 3-3 Lathe Grinding Assembly

pair of electrolyte disks (see Section 2, above) is then fitted to the drum body. Since the interior diameter of the step will vary with the dimension of the original tube stock and the drum wall thickness desired, each disk is custom fitted. The finished diameter of a disk is adjusted by gluing it to a handle, mounting in the lathe, and reducing to the desired dimension by grinding down the outside edge. A total clearance of about 0.005 inch (0.013 cm) is maintained between the o.d. of the disk and the i.d. of the step wall to allow for the brazing fillet. The drum body steps produced on the lathe grinding assembly have a radius at the bottom of the cut. In most cases, the inside corners of the disk edges are lapped in place to allow seating all the way to the bottom of the drum step. The desirability of this lapping procedure is still under investigation.

Several parameters in the machining operations can affect the quality of the final brazed drum assembly. Among those currently monitored for control purposes and correlated for process improvement potentialities are vendor's lot of tube stock, diameter of stock, overall wall thickness, sealing wall thickness, hole drill bit type, disk thickness, brazing fillet gap, lapping procedure (if any), and lapping compound used. Prior to release of a drum assembly for plating, the parts are inspected for chips or cracks and fit of disks to body. The body and disks are then engraved with unique part numbers to prevent any mixup in subsequent operations.

3.1.2 Manifold Tubes

All manifold tubes (used to distribute and collect gas from a set of drums in a given electrolyzer module) used in the construction of drum electrolyzers have been fabricated from 3/8 inch (0.95 cm) o.d. closed-end alumina tubes obtained from an outside vendor (McDanel Refractory Porcelain Company). The small gas port tubulation holes are drilled with the same equipment used for drum bodies, except that a hand feed is employed to avoid over enlargement of the holes. Quality control parameters are the composition and grade of the tubing and size of the holes as compared to the tubulation that will be brazed in.

3.2 PLATING

The ceramic components are plated to provide a wettable sur-

face that will lead the braze fillet metal into the locations desired. To insure a gas-tight fillet, the plate must be continuous over the area to be brazed, and it must remain adherent to the ceramic substrate under the brazing conditions used. The plate material used in electrolyzer components is platinum, applied by electroplating, using the basic procedure described in Refs. 2 and 3. The braze metal is gold (or its alloys) which dissolve the platinum plate. Therefore, another condition for successful brazing is that the plate be thick enough so as not to be completely dissolved in any given area prior to solidification of the fillet. Meeting these stringent plate requirements with a variety of ceramic substrate compositions, textures, and shapes has required close attention to substrate preparation; plating bath composition and history; and plating voltages, currents, temperatures and times. Despite all practical controls, electroplating remains, in part, an operator sensitive technique. To insure that a consistent plate quality is achieved, a series of post-plating quality control checks has been instituted.

The control procedure for plating zirconia entails inspection of the ceramic parts to insure that all areas to be plated have been buffed to remove any suface glaze. (Unbuffed, high fired ceramic surfaces can give poor adhesion and failure to plate.) The parts are then scrubbed using a mild abrasive (household cleanser) and wet wiped and rinsed prior to initiation of the plating procedure. Alumina substrates are treated likewise with the addition of a soak in mild sulfuric and then in nitric acid following the scrubbing. During the sensitization, extra bath liquid is forced through the holes to insure subsequent plating inside. The ease of plating inside the holes can vary with the type of drill bit employed. Electroplating is initiated at 4 to 5 volts, and after a continuous metallic film is obtained, the voltage is reduced to approximately 2 volts, to give a current density of the order of 10 mA/cm^2 and continued for about 20 minutes. The plate is then examined for color, coverage, and for absence of peeling or blistering. If judged adequate, the plate is rinsed and fired in air at a nominal 1250°C. If judged inadequate, the plating period may be prolonged, or the plate removed by buffing or sandblasting and the entire sequence reinitiated. After firing, the plating thickness is measured by weight gain and the adherence judged by scratch tests on plated areas which will be removed prior to brazing. If the weight gain is found to be below about 5 mg/cm^2, additional plating may be carried out. If the adhesion is poor,

the plate is removed and the sequence repeated. The exact plating currents and times will be varied slightly according to the performance on similar parts previously plated from the same bath. Plating bath records are kept, including the manufacturers' lots for both components and makeup additions. When a bath fails to give the desired plate, it is replaced. Each ceramic part is assigned a unique plating record number so that the results of future operations can be correlated with plating parameters.

3.3 SEALING

3.3.1 Drum Components

The history of the evolution of the electrolyzer module subunit into the present edge-sealed drum configuration has been documented in Ref. 2. Since this sealing configuration has been highly successful for the production of gas-tight subunits, no change in the basic design has been necessary. All work this year on drum sealing has been oriented toward improvements and standardization of the furnace brazing procedure. Our advances in the technology of sealing the drums to the gas manifold tubes (discussed below) have eliminated the necessity of sequential furnace brazing operations; thus, only one composition of brazing fillet material is required. Gold has been chosen as our standard braze material. It has a convenient melting temperature (1063°C) well above the operating temperature of the electrolyzer, but within the operating temperature range of ordinary wirewound furnaces. After melting, gold readily flows into the fillet areas, in contrast to non-eutectic alloyw, which melt over a temperature range and flow sluggishly. At the beginning of this year's program, however, two drums were successfully sealed using a gold-palladium braze (melting point ~1100°C). This approach was not pursued any further.

Our standard brazing procedure calls for the removal of all excess platinum plate from the ceramic parts by diamond wheel grinding or sandblasting. Plate is retained on the vertical surface of the drum step sealing wall, on the edge of the disks, and on a small area around each tube and wire hole, as well as inside the holes. Elimination of the excess plated area acts to keep the melted gold, during brazing, in the areas to be filled and avoids electrical shorting and fillets having reduced cross section. A circle of 0.020 inch

(0.05 cm) diameter gold is placed into each drum step and each disk is placed over this circle, taking care to pass the internal grid lead wires though their corresponding holes in the drum body. The gas port tubulations are inserted and a wrap consisting of 1½ turns of 0.020 inch (0.05 cm) diameter gold wire is placed around each wire and tube adjacent to the outside wall of the drum. The drum is then mounted on a ceramic jig (Fig. 3-4) with provisions for supporting the gas port tubes. A band of ceramic cement is placed around each tube and wire to keep the gold near the drum body. A small square of gold metal is placed on the edge of the drum to act as a visual temperature flag.

The jig is placed into a vertical exposed wire element tube furnace and supported so that the drum is centered in the furnace. Weights and a thermocouple are put into place and the furnace is sealed, with a view port at the top to allow observation of the flag and one wire or tube wrap. The temperature of the furnace is raised over the course of two to three hours to 1050°C. At this point, full furnace power is applied to raise the temperature quickly, in about two minutes, to approximately 1080°C at the thermocouple location. Melting times of the gold wrap and flag are noted and the furnace power is turned off close to ½ minute after complete melting of the flag. The temperature falls below the gold point rapidly, taking about one minute after power off. The rate of temperature fall decreases, taking overnight to approach room temperature. When cool, the drum seals are examined, taking note of whether the gold alloy braze has entered all the tube and wire holes and whether a continuous band of gold has been extruded around each disk seal.

The time-temperature brazing sequence described has been developed for zirconia drum bodies and a given furnace geometry. The tube and wire braze wraps are exposed to the incident radiation from the heating element, but the disk seal braze circle is inside the drum. The actual temperatures achieved at the sealing areas depend upon the several rates of heat absorption, emission, and conduction of the ceramic and metallic components involved. All sealing area temperatures must be high enough to allow the gold to flow, but must not be too high nor kept at temperature too long or the gold will completely dissolve the platinum plate. If an alternate ceramic is substituted for the ZrO_2 drum body (for instance, Al_2O_3) this time-temperature sequence is no longer applicable and all the braze material may not melt. On the other hand,

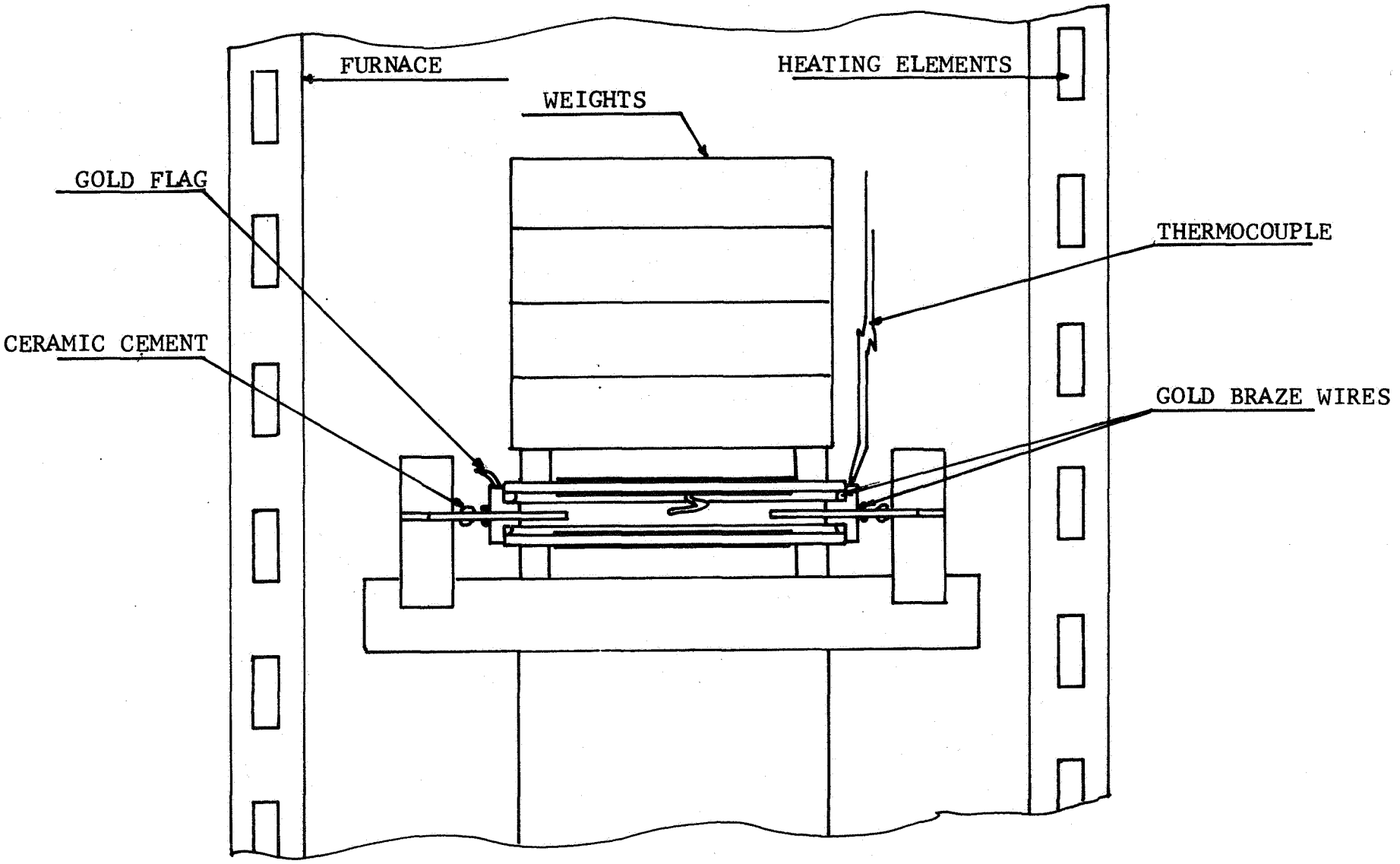

Fig. 3-4 Drum in Brazing Jig in Sealing Furnace

all mechanically sound zirconia drum bodies sealed this year, have been gas-tight provided the plating was applied using the improved procedures and control techniques described in subsection 3.2 above.

Several drum bodies were sealed this year employing an alternate furnace brazing philosophy. In this case, the furnace temperature is raised to only a few degrees above the braze melting point and held for a long period. The braze can dissolve the plate until the alloy solution becomes saturated at the furnace temperature, and then the alloy freezes. Basic requirements are that the final temperature rise be fast emough to allow all the braze material to flow before the alloying action is complete, and that the temperature control be accurate, steady, and uniform throughout the furnace. Advantages of this brazing technique are that the heat absorption and conduction rate of the several components become less important, the process may be more easily automated, and many drums could be sealed simultaneously in a large, uniform temperature furnace. A moderate size box furnace equipped with ceramic-shielded heating elements on four sides was used to try this brazing technique. The temperature distribution was not quite as uniform as was desired (heat leak through the door and back wall lowered the temperature on parts facing those directions below the gold melting point), however the drums were sealed successfully and the feasibility of the method has been demonstrated.

3.3.2 Manifold Assemblies

Furnace brazing of manifold assemblies and other non-drum seals have been described in Ref. 2. All electrolyzer modules through Z-12 were brazed together by insertion of the drum gas port tubulations directly into the manifold distribution tubes and brazing with the entire module assembly in the furnace. The braze material used was silver-gold alloy, or sometimes pure silver, to avoid raising the drums previously sealed with gold back to their original sealing temperature.

An advance in manifold sealing technology has been effected by the introduction of torch brazing for joining small metal tubulations. Both Pt-Ir and Au-Pd alloy tubes have been joined using gold as the braze material. In our current procedure, metal tube stubs are furnace brazed into alumina manifold tubes independently of the drums. The drum port tubulations are then torch brazed to the stubs on the manifold tubes to give a completed electrolyzer module. Several coupling

techniques have been employed. In the "large stub" method, the smaller 0.070 inch (0.18 cm) o.d. drum tubulations are slipped directly into larger 0.100 inch (0.25 cm) o.d. x 0.072 inch (0.18 cm) i.d. stubs on the manifolds. Small diameter tubulations have also been furnace brazed to both components, and then joined together by use of larger diameter coupling. The latter method requires two torch brazes per manifold connection. In our preferred "compound stub" method, each larger diameter coupling is first torch brazed to a smaller diameter manifold stub. The small ends of the compound tubes are then furnace brazed into the alumina manifold tubes. The drum-to-manifold joints are then made by a single torch braze per connection.

Furnace brazing of the joints in the manifold tubes is performed in a manner similar to that for the drum sealup. The platinum plate on the alumina manifold tubes is first checked for thickness and adherence. If deemed satisfactory, the excess plate is removed to leave a small area around each hole. Tubulation stubs are inserted with a wrap of 1½ turns of 0.020 inch (0.05 cm) gold wire adjacent to the plated area, the assembly is mounted in a special ceramic jig (see Fig. 3-5) and the brazing operation is carried out as described above for drums. Because of the length of the present style of manifold tubes (two feet long) no attempt has been made to furnace braze them using the "constant temperature" technique described above in sub-section 3.3.1.

3.3.3 Testing

Following each furnace or torch brazing run, the particular sub-assembly is tested for leaks at room temperature using the "$\Delta t/\Delta p$ test" described in Ref. 2. Due to the greater integrity and low leak rates provided by the current brazing techniques, the less sensitive water manometer version of the $\Delta t/\Delta p$ test has been completely superseded this year by the more sensitive dry gauge system. The "thermocycle" testing procedure formerly employed as a gauge of seal reliability has become unnecessary, since edge-sealed drums have shown no significant degradation in seal quality on reheating to brazing temperatures. In general, the brazed ceramic and metal assemblies now being produced exhibit a leak rate of the order of five times less than the "pass-fail" point of two minutes using the old water manometer version of the $\Delta t/\Delta p$ test.

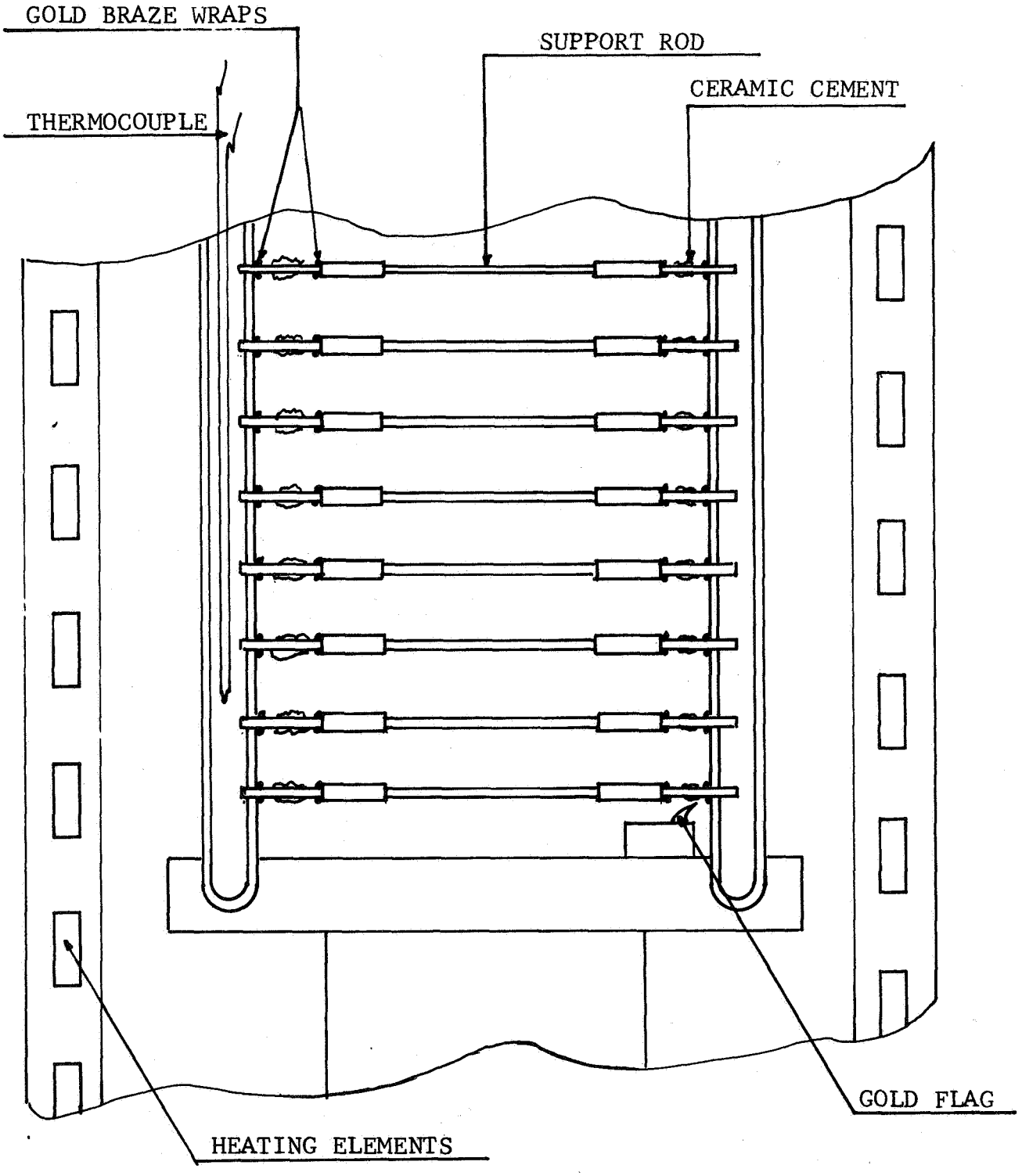

Fig. 3-5 Manifold Tubes in Brazing Jig in Sealing Furnace

3.4 ELECTRICAL LEADS

A gold alloy (96.5% Au, 3.5% Pd, by weight) has been successfully substituted for platinum in the 1 mm diameter electrical lead wires sealed into the zirconia drums. This change increases the electrical conductivity significantly (a factor of 3.2 at 883°C), thereby lowering voltage losses and reducing I^2R heating of the wires. (Such heating may have contributed to the cracking of drum bodies in two modules of the one-man unit discussed in sub-section 5.1, below.)

3.5 GAS FLOW

The question of equal distribution of gas flow to several drums in a Z unit has been a matter of concern, since a gradient in pressure along the manifold would starve the drums toward the end of the tube. An analysis using best estimate high-temperature gas properties confirms that the gas distribution is indeed uniform for the present design. The criterion for good manifold distribution is that the pressure drop at each exit should be at least ten times the pressure drop along the length of the manifold (Ref. 4).

The principal pressure losses are: 1) through the length of 7.1 mm diameter manifold tubing, 2) at exit and entrance of the 1 mm metal connecting tubes, and 3) though the length of the 1 mm connecting tubes. Pressure drop across the electrolyzer drums is negligible, since the flow cross section is relatively large.

The manifold tube flow has a temperature gradient from 25°C to nearly 900°C at the working end. Mean values of viscosity, density, and volume were calculated from published values for CO_2 and the perfect gas law. The pressure drop was then taken from the Fanning pipe friction equation,

$$\Delta p = \tfrac{1}{2}\rho V^2 \, f\left(\frac{L}{D}\right)$$

where the friction factor, f, is obtained from friction factor vs. Reynold's number curves, again taken as the arithmetic mean along the manifold. The approximate pressure drop for a total flow of 600 ml/min is then 0.035 inch of water in the manifold.

The pressure drop along the 1 mm diameter metal tubulation was likewise taken from the pipe friction equation, with properties at 900°C and 1/6 of the total flow (for a six-drum module). This drop, the most significant part of the total flow loss, is 0.36 inch of water for each tube. Each drum has two tubes.

Entrance and exit losses at the ends of the 1 mm tubulation are taken from the well-known flow loss equation

$$\Delta p = \tfrac{1}{2}\rho V^2 \, C_D$$

where the coefficient, C_D, is assumed to be 0.5 for square-edged entrances. This loss is 0.032 inch of water at each end and there are four ends for each drum.

The total pressure drop per drum is calculated as 0.808 inch of water (two tubes and four ends). This total back pressure per drum is the effective exit drop "seen" by the manifold in regard to distribution. The ratio of exit drop to manifold drop is thus 0.808/0.032 = 23 which is well above the minimum of 10 suggested by Perry (Ref. 4). We are thus assured of uniform flow distribution in the present design. Care has been taken in the assembly process to avoid tubing kinks, ragged, edges, and brazing plugs, which would vary the flow to individual drums. It should be noted that the major pressure drop is along the length of the 1 mm tubing.

Pressure drop measurements in the laboratory gave approximately three inches of water for the six-drum modules. This included the flow through several feet of connecting tubing and fittings. The discrepancy with the calculated pressure drop is due to this factor as well as approximations in entrance coefficients and gas property assumptions. Nevertheless, the calculated values are useful in comparing relative pressure drops in various parts of the system, as in the manifold to metal tubing ratio, above.

A transparent Plexiglas model of a drum was prepared in order to observe internal circulation of fluid at room temperature. Water was used as the model fluid, with a stream velocity chosen to match the Reynold's Number of high-temperature gas in the real drum. A stream of colored ink was injected into the fluid for flow visualization just ahead of the inlet tubing. The model included complete grids and lead wires, cemented to the disk inner faces.

The tubing arrangement in which the entrance tube faces a diametrically opposed exit tube showed very little mixing in the drum. The fluid moved across the drum in a jet which impinged on the exit tube.

A variation was made by turning the entrance tube 90°, forming a smooth elbow inside the drum. This induced some mixing, but mostly in the half of the drum toward which the elbow pointed.

A second variation was made by capping the end of the inlet tube with gold braze and drilling two lateral holes 0.5 mm in diameter across the tube. This resulted in two streams which swept around the periphery of the drum with substantial swirling. Entrance nozzles of this type have been incorporated in the six-drum electrolyzer, Z-17, and in all subsequent electrolyzers.

A standard procedure has been developed for insuring that the pressure drop through all double-hole drum entrance nozzles in a given electrolyzer module will be substantially equal. After fabrication of the nozzle, and before sealing it into a drum, gas is passed through the nozzle and the flow rate noted for a defined pressure drop. The size of the lateral holes is then carefully enlarged, if necessary, until the flow rate for a set of nozzles is the same. These flow rates are recorded and become part of the record kept on each drum (along with the plating, brazing, and test histories and results) for possible future correlation.

3.6 SUMMARY OF ELECTROLYZER DEVELOPMENT

Several major improvements in electrolyzer assembly procedure have been made during this contract year. The use of torch brazing for final manifold connections has been described above in sub-section 3.3.2. The fabrication of all electrolyzer modules this year has entailed some variation of the torch braze method. These electrolyzer modules are listed in Table 3-1. All of the drums (with one exception noted below) have been assembled using the new higher conductivity gold-palladium alloy leads described in sub-section 3.4.

The design of drum gas port entrance nozzles has evolved during the course of the year. The particular design used in a given module is noted in Table 3-1 and described in sub-section

Table 3-1

ELECTROLYZER CONSTRUCTION DETAILS

Module Number	Drum Numbers	Disk Sc_2O_3 Content	Grid Style	Nozzle Style	Manifold Connection	Electrical Wiring	Furnace Geometry	Electrolysis Test Number
Z-13	F-206 F-207	7%	K-1D	90^{o} Inside Inlet Elbow	Special*	Series	Vertical	J-7
Z-14	F-203 F-205	7%	K-1C	Plain Tube	Large Stub	Parallel*	Vertical	J-6
Z-17	F-209 F-210 F-211 F-213 F-216 F-218	7%	K-1D	Double Hole Inlet (DHI)	Large Stub	Special* Series	Special* Horizontal	J-10
Z-19	F-220	7%	K-1E	DHI	Compound Stub	Series	Horizontal	J-14
Z-20	F-227* F-229*	8%	K-9 K-12	DHI	Large Stub	Series	Horizontal	J-15
Z-21	F-240	8%	K-14	DHI	Compound Stub	Series Aux. Electrode	Horizontal	J-16
Z-23	F-247	8%	K-17	DHI	Large Stub	Parallel*	Horizontal	J-18
Z-24	F-232 F-235 F-237 F-238 F-242* F-244 F-245 F-246	8%	K-13 K-13 K-14 K-16A K-16B K-16D K-14 K-16E	DHI	Compound Stub	Series Auxiliary Electrode	Horizontal	J-17

* See text for description of details

3.5. Wilkalloy 1651 alloy (a hardened gold-palladium alloy patented by The Wilkinson Company) has been used for all gas port tubulations in drums fabricated this year as an economy measure and does not reflect a commitment to this alloy as a "material of choice" for future space oriented designs, where platinum-iridium alloys are probably more suitable. Many different grid-electrode styles have been tested through their incorporation into the drums of the several electrolyzer modules. The particular style employed on each drum is noted in Table 3-1. The details of each grid style are given below in Section 4. Certain modifications in the manner of electrical interconnection of the disks and drums in some of the modules have been made in addition to the standard series method employed in the one-man electrolyzer. The electrical wiring method is noted in Table 3-1, and exceptions to the standard series method are explained in the list of specific electrolyzer details given below in Section 5.

With the use of torch brazing, the total length of connecting metal tubulation between the alumina manifold tube and the drum body was increased to about 3.5 cm. This has allowed room to make the torch braze without melting out the previously furnace brazed joints. The increase in length of tubulation together with the use of the softer Wilkalloy 1651 alloy for the drum gas ports has led to reduction in the rigidity of the overall connection. In the case of the one-man electrolyzer modules (and earlier drum-type electrolyzers) the drums were adequately supported directly from the manifold tubes through the stiffness of the short all Pt-Ir alloy connections. It was, therefore, convenient to operate the modules, for test purposes, with the manifold tubes in a vertical configuration. (See, for instance, Figs. 3-1 and 6-4 of Ref. 2.) Operating experience with the first two torch brazed electrolyzers demonstrated that the less rigid Au-Pd tubulations were subject to creep through action of the weight of the drums at electrolyzer operating temperature. In one case the resultant sag was enough to allow electrical shorting between the drums. A laboratory solution to this problem was the development of the horizontal furnace testing geometry shown in Fig. 3-6. Each alumina manifold tube is rigidly held in a horizontal position by virtue of its passing through a port in the mullite envelope closure plate at one end, and through a special Lava A jig plate at the other end. The drums are supported on the manifold tubes by Fiberfrax pads to avoid direct ceramic-to-ceramic contact. The exterior drum tubulation elbow angle was changed (during sealup of the drums)

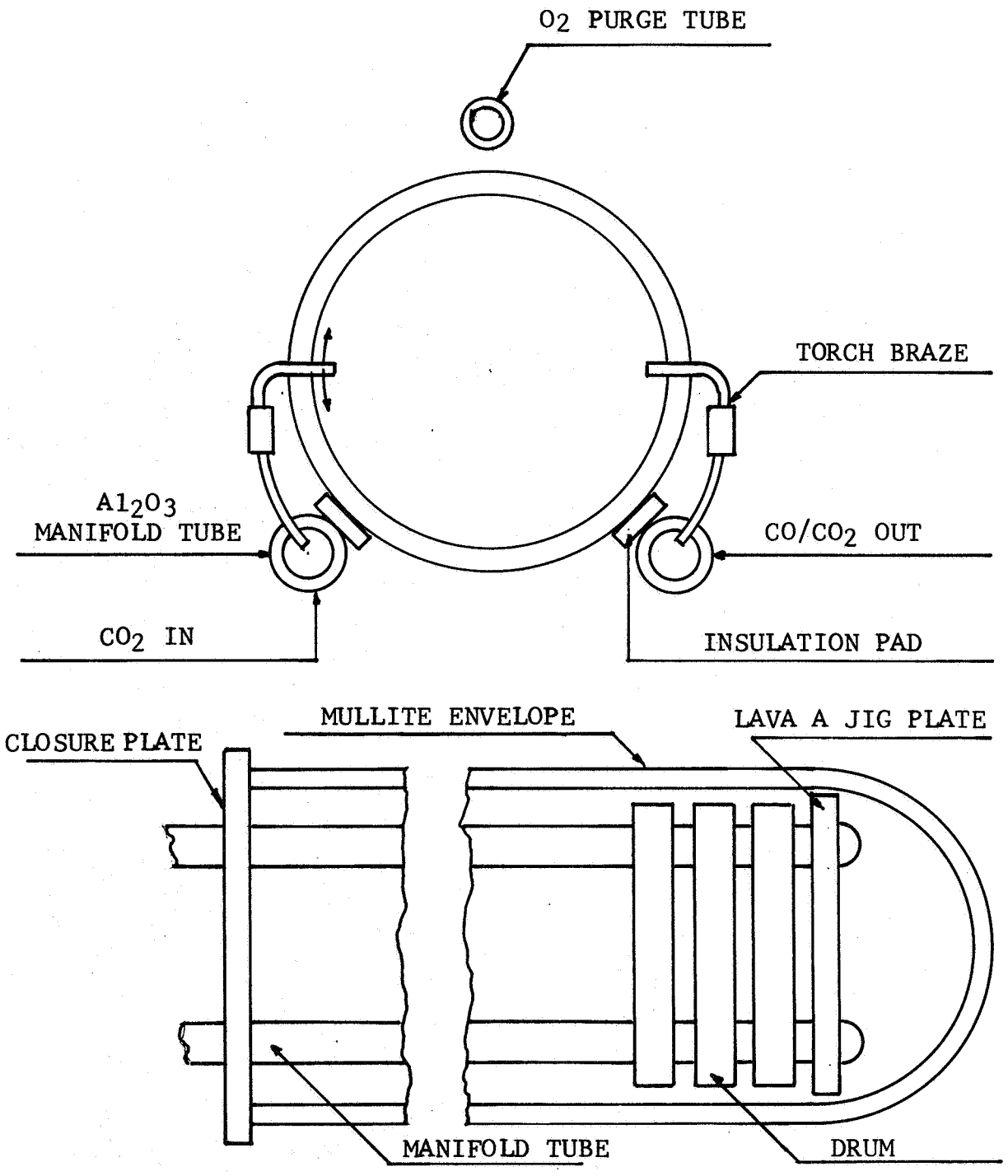

Fig. 3-6 Configuration of Drums
in Horizontal Furnace During Operation

so that both elbows face the same direction. This change has facilitated the manifold-to-drum assembly for torch brazing. The present arrangement is considered a laboratory solution only, since ultimate development will require a mounting for drums and manifolds to withstand omnidirectional vibration and acceleration forces.

The drum bodies used to construct the electrolyzer modules in Table 3-1 have all (with the exception of Z-20, see Section 5 below) been fabricated from calcia-zirconia stock to an overall height of 0.400 inch (1.0 cm) and all have the edge seal configuration (see sub-section 3.3.1) using gold as the brazing fillet.

3.7 CATALYTIC REACTOR AND RECYCLE LOOP

The contemplated CO_2-H_2O electrolysis system containing two separate banks of electrolyzers (for recovering oxygen from carbon dioxide and metabolic water), pumps, recycle loops, H_2O-H_2 separator, and a catalytic reactor is shown schematically in Fig. 3-7. The separator and its recycle loop may not be required, since it has been shown (Ref. 8) that water vapor can be electrolyzed much more readily than carbon dioxide (at higher current densities with negligible polarization losses at the cathode). It should be possible to obtain a sufficient degree of conversion per pass through the water electrolyzer bank so that the wet hydrogen could be dumped or otherwise utilized without a need for a recycle loop, separator or high-temperature water vapor pump. In contrast, the CO_2 recycle loop and catalytic reactor are necessary to carrying out the chemical reactions required for complete oxygen recovery. These reactions are

$$\text{Electrolyzer:} \quad CO_2 \rightleftarrows CO + \tfrac{1}{2} O_2 \qquad (3\text{-}1)$$

$$\text{Reactor:} \quad CO \rightleftarrows \tfrac{1}{2} \underline{C} + \tfrac{1}{2} CO_2 \qquad (3\text{-}2)$$

The H_2 and H_2O shown in parantheses in Fig. 3-7 represent small concentrations of these species carried around the recycle loop to catalyze the cathode reaction in the electrolyzer and reaction 3-2 in the reactor.

Reaction 3-2 (the Boudouard equilibrium) has been extensively studied by many investigators as to effects of various catalysts, temperatures, and gaseous impurities in the CO. Iron,

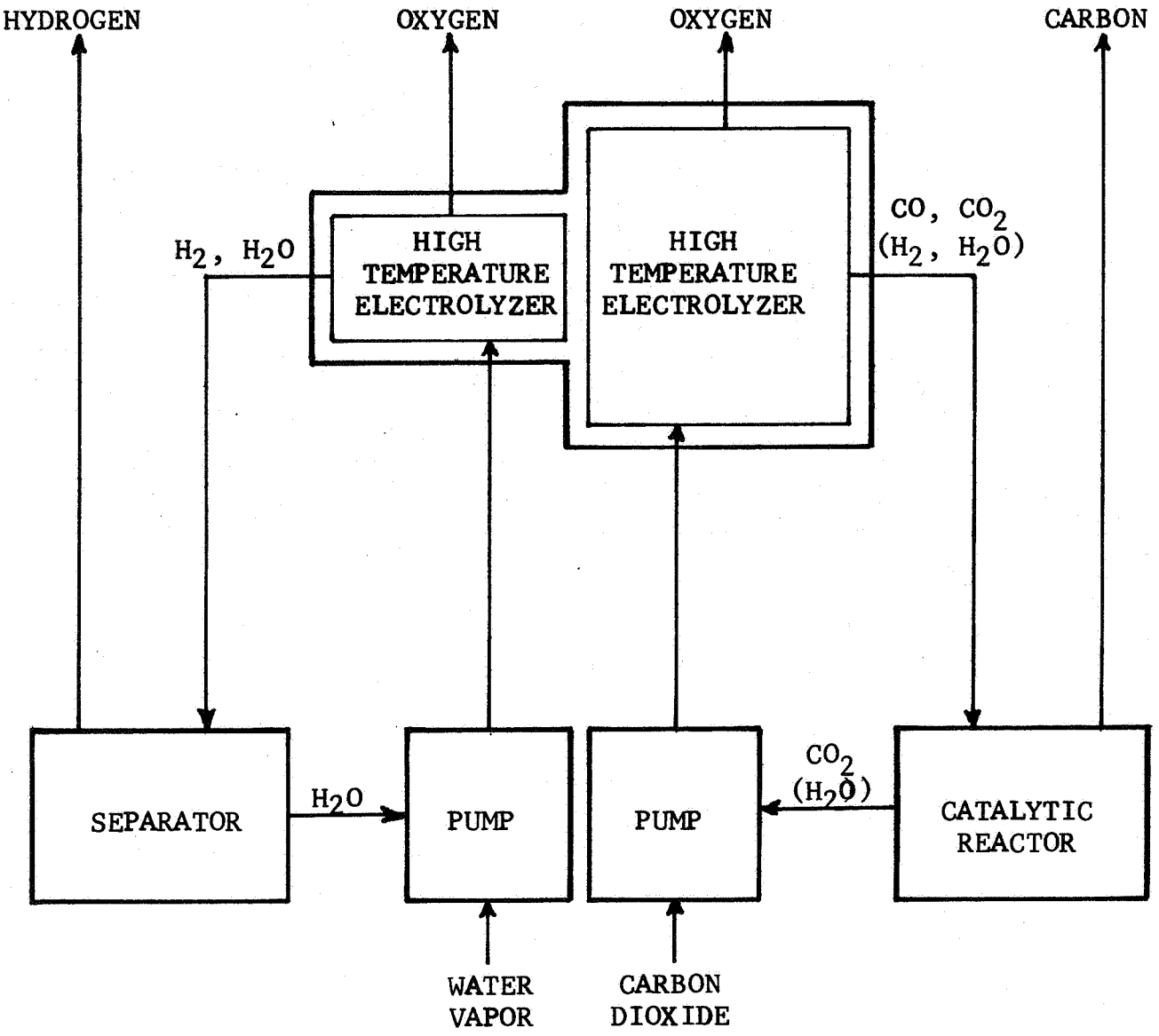

Fig. 3-7 Carbon Dioxide-Water Electrolysis System

cobalt, and nickel have been found to be the best catalysts. Reaction rates, properties of the carbon that is formed, and the effect of H_2 and H_2O in increasing both the reaction rate and the ultimate amount of carbon formed with a given mass of iron catalyst are given in Refs. 5, 6, and 7.

During the first two years of this contract, canister-type reactors using low carbon steel as the catalyst were operated with CO from cylinders and also with the exit CO-CO_2 streams from CO_2 electrolyzers operating at total currents in the range 12 to 127 amperes. Typical percent conversion for CO-H_2 are shown in Fig. 3-8 (see Section 4 of Ref. 1). The present conversion exceeded 80% after a 50 hour induction period. Percent conversion of CO to C and CO_2 is calculated as follows:

$$\% \text{ conversion} = \frac{(j_{CO} \text{ into reactor}) - (j_{CO} \text{ from reactor})}{(j_{CO} \text{ into reactor})} \times 100 \qquad (3\text{-}3)$$

where j is the flow rate in ml/min.

In the test runs of reactor operation using CO-CO_2 from operating electrolyzers, the reactor effluent was vented and not recycled. The flow system was shown in Ref. 2, p. 82. The degree of conversion of CO to CO_2 and carbon in the reactor was determined periodically during each run by gas chromatographic analysis of the CO-CO_2 stream leaving the electrolyzer with only a 53% CO content, the CO removed during passage through the reactor was found to be 32% as calculated from Eq. 3-3. This extent of CO disproportionation is within the range of acceptability for recycle loop operation at a reasonable recycle ratio; however, percent conversion would be significantly increased by operating the electrolyzer at higher CO/CO_2 output ratios.

Electrolyzer operation at effluent CO concentrations as high as 92% has, in fact, been achieved. Unit Z-23 (one drum) has run for 45 days at output CO concentrations greater than 60% including one day of operation at 92% CO. (Variations in CO concentration were the result of experimental changes in the CO_2 input rates.) This unit continues in operation at ~80% CO output. Unit Z-21 (one drum) was operated for ten days with output CO about 60%, including one day at 82%. Unit Z-24 (eight drums) has run for 46 days in the range 58 to 62% CO and continues in operation at ~60% CO output concentration. Operating data for these electrolyzers is given in greater detail in Section 5.

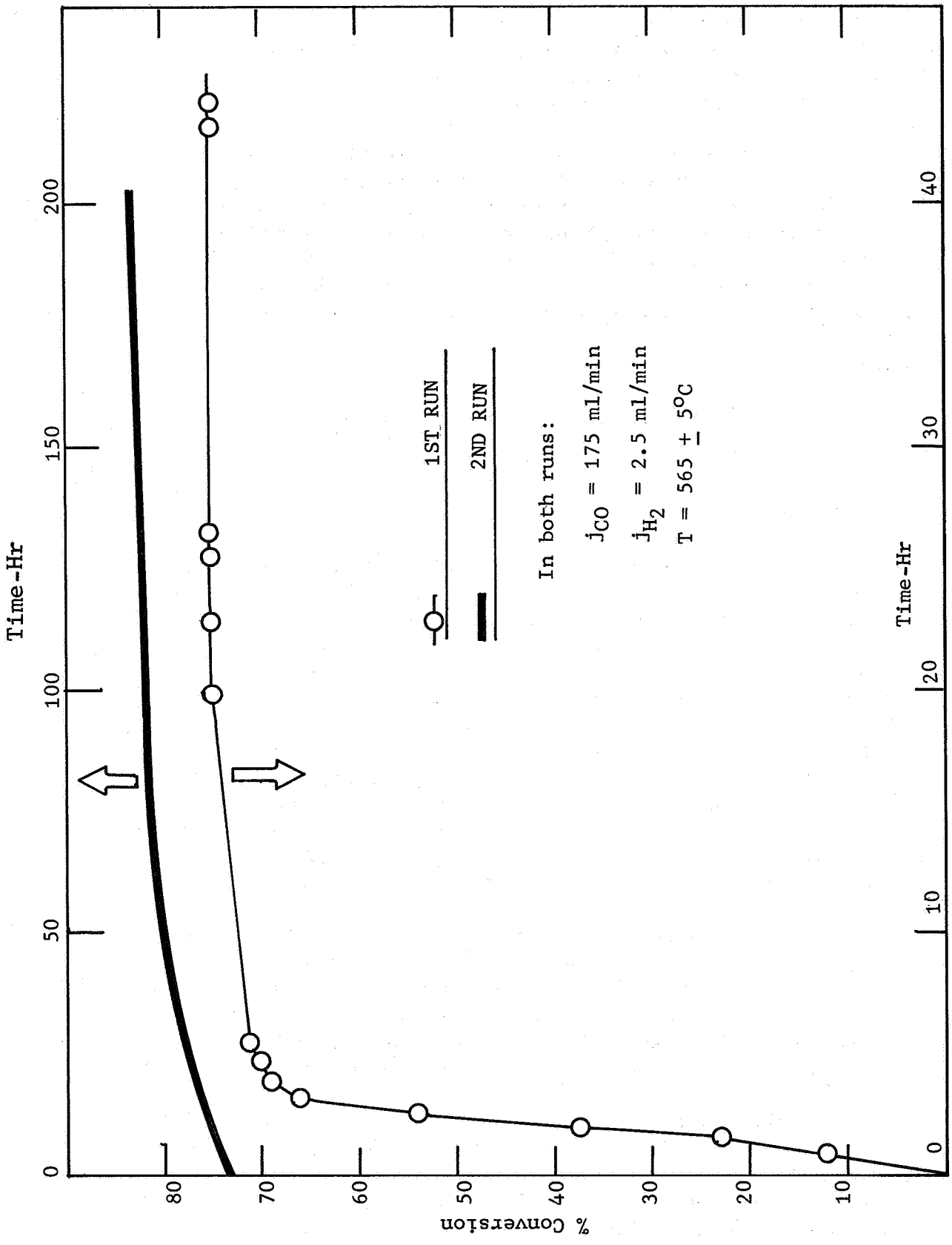

Fig. 3-8 Efficiency of the Steel Reactor as a Function of Exposure Time

Inasmuch as an adequate degree of conversion can be obtained with low carbon steel catalyst, no further work was undertaken to find a better catalyst. Some catalytic tests were made, however, to aid in selecting materials for a canister-type reactor designed for easy removal of the light weight canister filled with carbon. This reactor design requires high catalytic activity within the removable cartridge but little or no activity at the fittings, cartridge exterior, or cartridge housing. Results of these tests, shown in Table 3-2, indicate that several alloys are available for these parts.

Table 3-2

MATERIALS - CARBON FORMATION AT 550°C

IN CO STREAM FOR 96-HR EXPOSURE

METAL	WT GAIN (%)
Aluminum 6061	0.045
Inconel 600	0.0
Stainless steel 17-7PH	0.0
Copper - 1% lead	0.0
Low carbon steel	3.9

Section 4

ELECTRODES AND GRIDS

4.1 GENERAL

The components of the electrical circuit of each electrolyzer described in this report and previous reports of this contract have been termed "electrical lead wires," "grids," and "electrodes." The electrical lead wires connect the power supply to the end cells of a multi-cell unit and provide a current path between cells. The lead wires connect to a current distribution element on each electrolyte disk consisting of a pattern of wires, the grid, the principal purpose of which is to distribute the current uniformly over the cell area without excessive voltage drop. The electrode is the porous electronically conducting film present as a layer on the surface of the electrolyte. It provides sites for the electrode reaction; electronic conductivity at the three-phase interface of gas, electrode, and electrolyte; sufficient catalytic activity to minimize activation overvoltage; and gas permeability to minimize concentration overvoltage. The electrode must also be mechanically and thermally stable during cell operation which imposes requirements of matching the coefficient of thermal expansion of the electrolyte to a reasonable extent, low vapor pressure, low surface mobility, and chemical stability in the gas atmosphere of the cell.

4.2 PREVIOUS DESIGN - PROBLEM AREAS

The grid style used in all drums through F-191, and incorporated in electrolyzer modules through Z-12 (designated as style K-1A), consisted of a circle of fine platinum mesh with a circle of 0.5 mm (0.020 inch) diameter platinum wire at the periphery. A piece of 1.0 mm (0.040 inch) platinum wire was welded to one point on the 0.5 mm (0.020 inch) wire to carry the current to the grid. The current leads of the grids on the two sides of a single electrolyte disk were 180^{o} apart to minimize concentration of the current at any one place on the cell. This type of grid is shown (scale X 2) in Fig. 4-1. The mesh is expanded platinum foil of 0.1 mm (0.004 inch) original thickness having diamond shaped openings (300 per square inch) 0.125 inch by 0.060 inch.

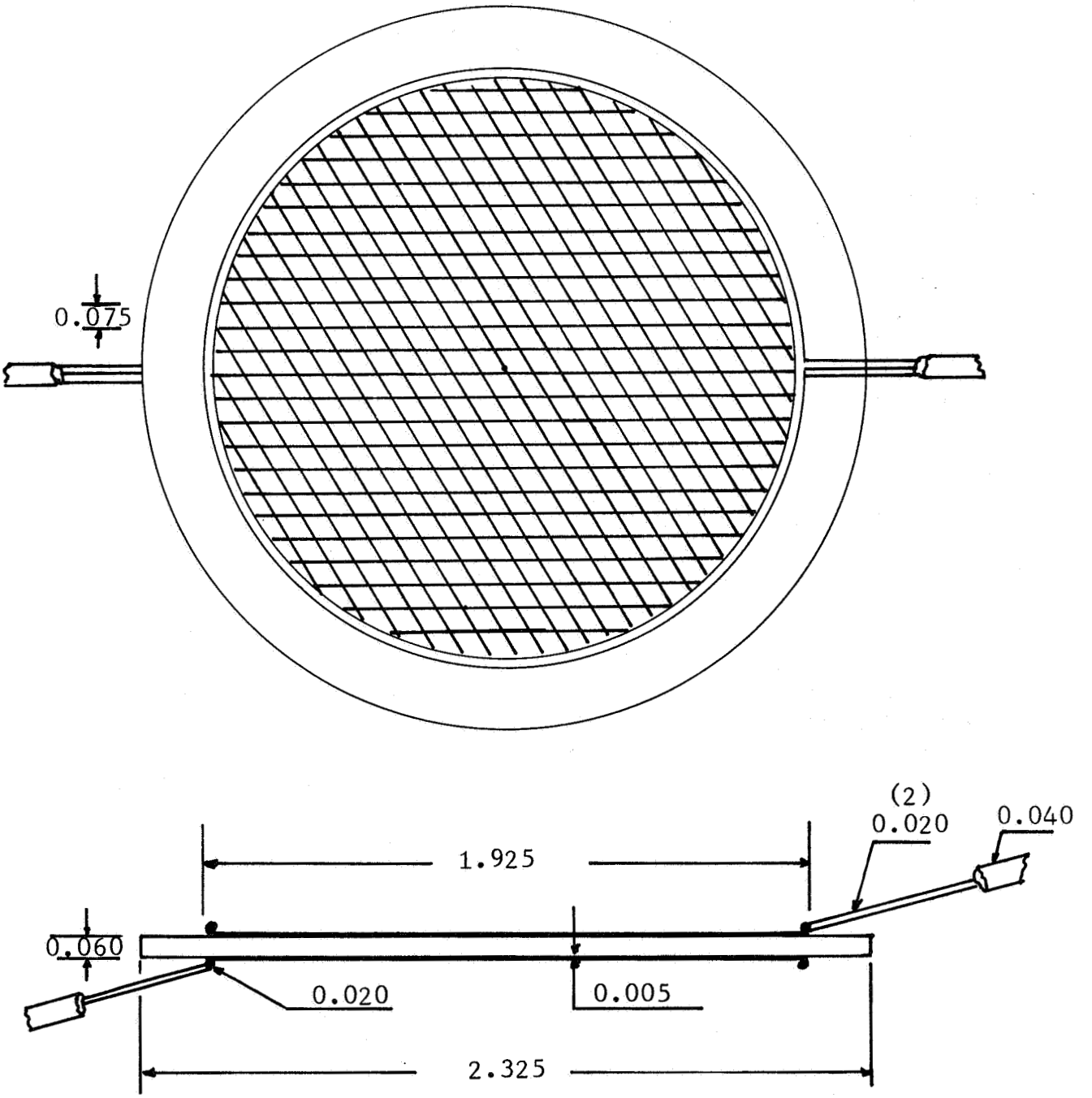

Fig. 4-1 Disk with Grid Style K-1A
(Twice Actual Size, Dimensions in Inches)

The electrode structure associated with the K-1A grid consists of platinum paste fired on at a nominal 1250°C.

This electrode-grid design has been found marginal for operation at an electrode area as large as 20 cm^2 and a current density as high as 200 mA/cm^2, although it was adequate for 5 cm^2 and 100 mA/cm^2 (Ref. 2). The problems of poor electrode and grid adhesion on the $CO-CO_2$ side and degradation of the electrolyte with eventual increasing porosity and cracking that were observed during the operation of 8 to 42 A electrolyzers at current densities in the range 175 to 200 mA/cm^2 led to a number of variations in design of the electrode structure, materials, and method of application to the electrolyte disk. Additionally, much greater attention was given to each step involved in making the electrode structures in order to improve the uniformity of cells of a particular design. Control of uniformity had not been very good previously as shown by the great differences in behavior of the cells in several of the electrolyzer modules described in Section 5 (for instance, units Z-10, Z-11, Z-12, Z-13, and Z-14). On the other hand, many cells did not exhibit symptoms of electrode-electrolyte degradation at 175 to 200 mA/cm^2 during prolonged CO_2 electrolysis. Problems with uneven current distribution are believed to be the cause of much of the performance and lifetime degradation. Modifications of the K-1A grid design were made in which the platinum mesh was retained but additional wires were added to reduce the IR drop across the grid.

4.3 OPEN CELL ELECTROLYSIS TESTS

Concurrent with rigorous, but slower, evaluations of electrode-grid structure that are provided with the normal operation of sealed-drum electrolyzers, a series of open cell tests was undertaken to screen the utility of advanced and "exotic" designs. In these tests, regular electrolyte disks are provided with electrode-grids and electrolysis is carried out in oxygen and carbon dioxide atmospheres with unsealed cells open to the same gas atmosphere on both sides.

A cell in which both grids were type K-1B of Fig. 4-2 and another cell with grids of type K-1C were run simultaneously in oxygen. These grids had 0.5 mm (0.020 inch) Pt wire at the periphery of the Pt mesh and the other wires were 9.65% Au, 3.5% Pd wires of 0.75 mm (0.030 inch) diameter. Current was passed at 1, 2, 3, and 4 A per cell in each direction at tem-

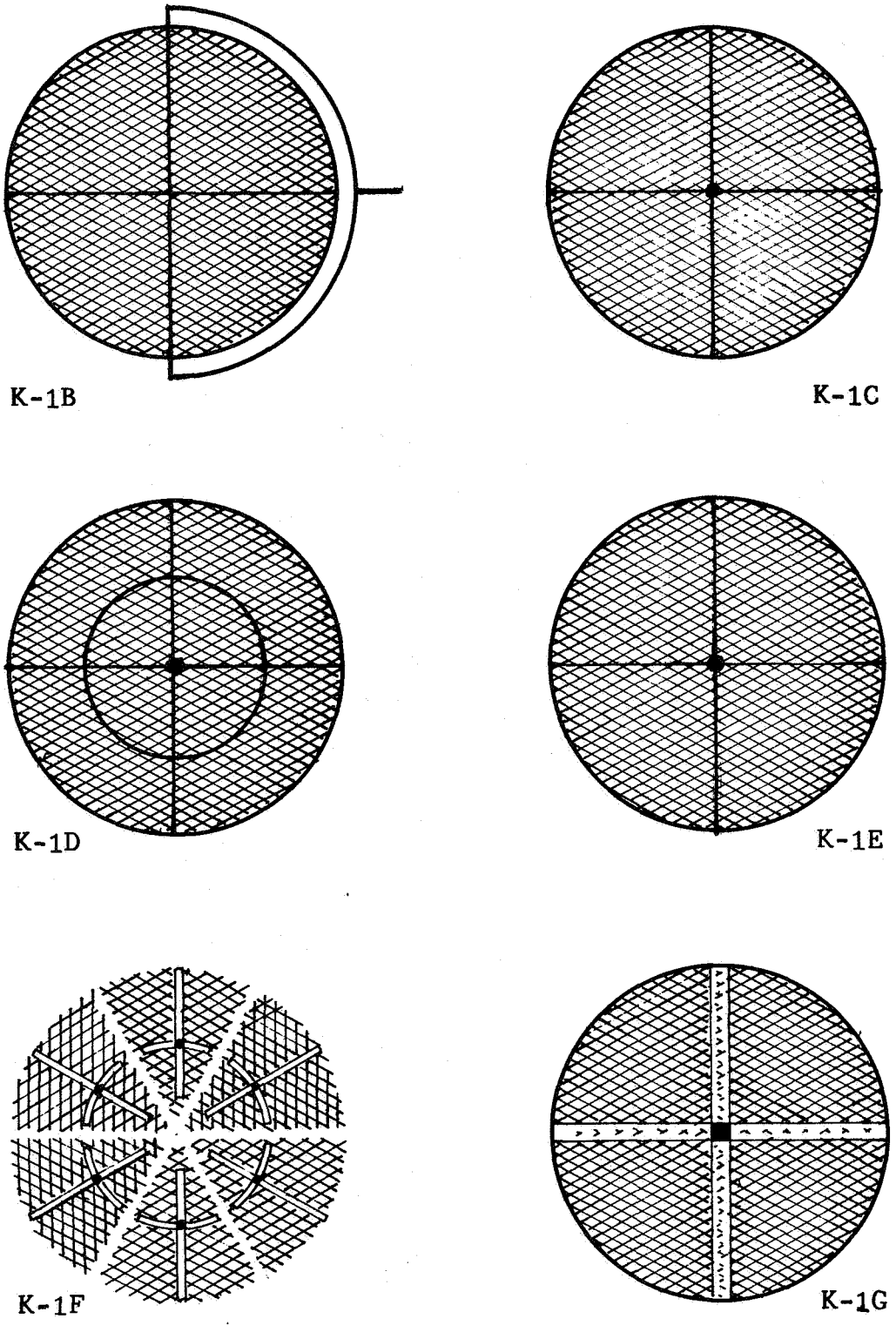

Fig. 4-2 Modifications of Grid Style K-1A

peratures in the range 850 to 890°C over a total period of 45 days (1080 hr). At a current of 4 A per cell (200 mA/cm^2), the initial and final voltages were 0.992 and 2.20 V for grid K-1B and 0.942 and 2.05 V for grid K-1C. Examination of the disks after termination of the electrolysis run disclosed poor adhesion of one grid of each type and discoloration of the electrolyte in the region of the gold alloy wires. These observations, combined with the high voltages that were required for electrolysis of oxygen, suggest that the current was distributed poorly and was concentrated near the gold alloy wires.

A series of seven electrolyte disks was prepared in which the two grids of each disk were the same. The styles were K-1E, K-1F, and K-1G of Fig. 4-2, and K-1H, which is described below for disk G-85A. One disk had K-1G grids and two disks of each of the other grid types were prepared. In addition to variations in grid design, there were changes in the method of electrode preparation and in the way that the grids were attached to the electrodes. These cells are summarized as follows:

G-107A	Style K-1E, all platinum wires, platinum paste electrodes
G-120D	Style K-1G, disk was electroplated with platinum in the shape of a cross inside a circle, grid of the same type as K-1C was then gold brazed to the plated area and platinum paste was applied after the brazing operation
G-97B	Style K-1F, six individual grids of platinum mesh each containing a cross of gold alloy wire
G-85A	Style K-1H, first electrode layer is electroplated platinum, then two layers of platinum paste; the grid is the same as for K-1A
G-84E	Same as G-85A
G-120TE	Same as G-107A
G-122A	Same as G-97B

The seven cells. open to the same gas atmosphere on both electrodes, were wired in series with provision also for individual

operation and placed into electrolysis operation in oxygen. After twelve days (288 hr) of oxygen electrolysis at currents up to 10 A per cell (500 mA/cm^2), the current was changed in 2 A increments to determine the current-voltage characteristic of each cell. These data are shown in Table 4-1.

Table 4-1

RUN J-11 CURRENT-VOLTAGE RELATIONSHIP
FOR OXYGEN ELECTROLYSIS AT 870°C

	CELL VOLTAGE (V)						
I (A)	G-107A	G-120D	G-97B	G-85A	G-84E	G-120TE	G-122A
2.0	0.850	0.708	0.401	0.414	0.453	0.490	0.759
4.0	1.490	1.888	0.688	0.723	0.798	0.848	1.290
6.0	1.85	1.475	0.885	0.946	1.073	1.111	1.64
8.0	2.05	1.64	1.012	1.097	1.279	1.291	1.86
10.0	2.18	1.74	1.091	1.225	1.63	1.401	1.99

The oxygen was replaced by CO_2 and the cells were run for three days at 4 A (200 mA/cm^2) and then for one day at 8 A (400 mA/cm^2). Examination after the electrolysis run disclosed that most of the disks were blackened and cracked and the grids on the cathode side were only loosely adherent. Areas near the highly conducting gold alloy wires were particularly affected by these problems. Disks G-85A and G-84E in which the first electrode layer was electroplated were better than most of the others. It was concluded from this experiment that an electroplated initial platinum layer was superior to platinum paste and that the grid designs incorporating the gold alloy wires distributed the current non-uniformly.

Another electrolysis experiment, using seven unsealed cells in both oxygen and carbon dioxide, was conducted to test electrode-grid styles using gold as the electrode paste, as the grid, and in various combinations thereof, in an effort to improve uniformity of current distribution and reduce the IR drop by increasing the electrical conductivity of the porous metal layer above that of platinum. This objective was not attained. Conversely, electrode-grid combinations employing gold paste exhibited cell potentials greater than a volt for oxygen transfer even at low current densities (<100 mA/cm^2). The dramatic contrast between the behavior

of platinum and gold electrode layers can be ascribed to severe polarization effects at the gold electrode. Grids that were first furnace brazed to a base layer of platinum plate on the disk and then gold pasted were more adherent than the others although the cell voltage was high, presumably because of the presence of gold over the entire electrode surface. The conclusion that was drawn from this experiment is that gold is not suitable as an electrode, even for electrolytic oxygen transfer.

4.4 SEALED DRUM ELECTROLYSIS TESTS

Electrode-grid styles K-1C and K-1D were employed for electrolyzer modules Z-13, Z-14, and Z-17 (operating data for these units are given in Section 5). Both of these styles (see Fig. 4-2) incorporated the platinum mesh grid and platinum paste electrodes of the original style K-1A with the addition of an overlay of 0.5 mm (0.020 inch) Au/3.5 Pd wires spot welded to the platinum grid. Examination of drums from these modules, after being electrolyzed to failure, have revealed several common characteristics. Platinum paste from the electrode has disappeared from the immediate vicinity of the gold alloy wires, presumably through a reaction which takes place to deposit a dark layer underneath these wires. The electrode-grid system is otherwise unaffected on the oxygen sides of the electrolyte disks. The bulk of the platinum paste is firmly attached to the disk surface, and the grid is adherent. On the reducing side of the disk, degradation is more severe. In addition to the disappearance of electrode paste adjacent to the gold wires, the grids have become dislodged from the electrolyte surface along with any residual platinum paste. The disks exhibit dark patches of varying size on the reducing side and may contain areas where the electrolyte ceramic has become porous and crumbly. When the dark or crumbly patches penetrate through to the other side (oxygen side) of the disk, failure occurs. Failure may take place through seepage of internal drum gas through a porous area, or the electrolyte disk may crack through the affected zone. Cracks in the electrolyte can propagate through the edge seal and cause fracture of the drum body. The drum body usually fractures along a weak zone, such as the gas port tubulation holes or the lead wire holes, which themselves may have been weakened due to electrolytic action (as evidenced by darkening of the drum body ceramic in the vicinity of the lead wire holes). Drums which have not failed, taken from the same electrolyzer modules, exhibit

all the characteristics described above, except that the dark or crumbly zones have not penetrated all the way through the electrolyte disks.

Since the electrode-grid combination used on the three electrolyzers (Z-13, Z-14, and Z-17) were substantially the same, the great increase in operating lifetime (~350 hr for Z-13 and Z-14 to more than 2000 hr for Z-17) must be ascribed to other factors, such as the reduction in current density (approximately 200 mA/cm^2 for Z-13 and Z-14 down to 100 mA/cm^2 for Z-17).

The electrode-grid style of the one drum electrolyzer Z-19 was K-1E (shown in Fig. 4-2). This drum was constructed to determine the relability and operating characteristics of a grid design intended to improve current distribution over the cell faces. Expanded platinum mesh with 0.5 mm (0.020 inch) peripheral platinum wire rim was fired to the electrolyte faces with platinum paste, as in previous electrodes. Current density concentration was changed by tapping the peripheral rim at four points with 0.5 mm platinum lead wires which were looped away from the electrode to a welded connection with a 1 mm gold alloy wire main lead. After over 1000 hours of electrolysis at 100 mA/cm^2, where the cell potentials remained at steady, low values (in the range 1.4 to 1.5 volts) the test was terminated due to an internal lead wire short. Examination of the cells revealed no deterioration of any kind. The inner grid-electrodes were still firmly attached. Comparison of cell potentials with those of Z-17 after 1000 hours showed that those of Z-19 were significantly lower. Tentative conclusions that can be drawn from the operation of this one-drum unit are that platinum current distribution wires are superior to gold alloy, and that the value of each cell potential is one of the most important guides in the selection of electrode-grid designs.

The cells of electrolyzer unit Z-20 which had special drum bodies (described in sub-section 5.5), were both fitted with all platinum grids in which the current path from the electrical lead is to the center of the electrode on one side of the cell, and from the perimeter of the electrode on the other side, as shown in Fig. 4-3. In style K-9 the grid was furnace brazed with small pieces of gold foil to seven small spots of platinum plating on the surface of the disk. The electrode consisted of layers of gold and platinum paste. In style K-12 the entire electrode surface of the disk was plated

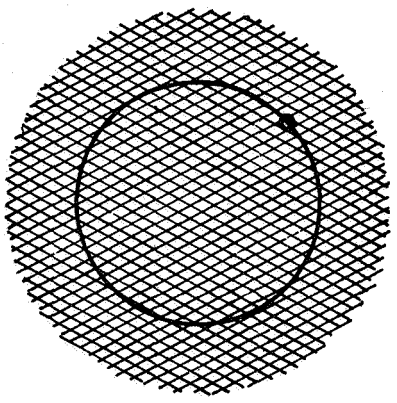

K-19

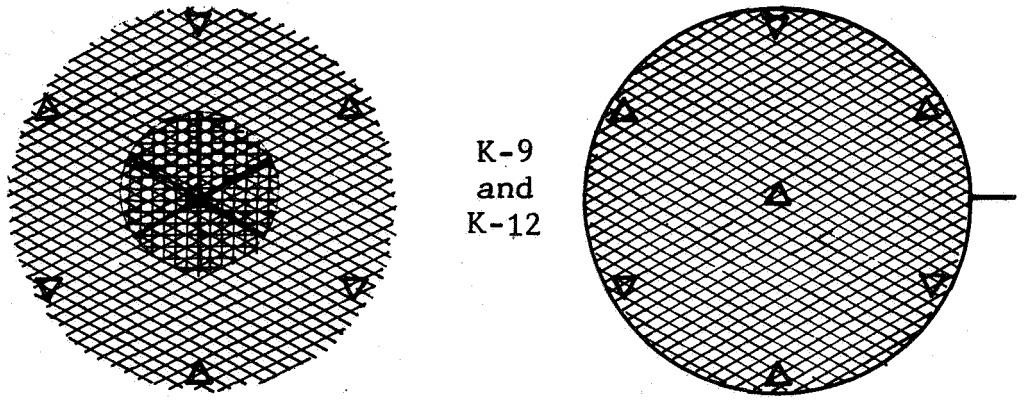

K-9
and
K-12

Fig. 4-3 Grid Styles K-9, K-12, and K-19

with platinum, the grids were brazed on, and then platinum paste (no gold paste) added. The conclusion with respect to the unsuitability of using gold in the electrode (determined concurrently in the open cell tests described above in subsection 4.3) was confirmed when the drum with the K-9 electrodes failed after about 1000 hours of electrolysis. The use of hydrogen on the CO_2 side probably served to extend the life of this drum over what might have been expected if only 3% water vapor had been employed. All of the degradation processes (observed in Z-13, Z-14, and Z-17) were in evidence for this drum. On the other hand, the drum with the K-12 electrode style showed very little evidence of degradation. The operating cell potentials of this drum were intermediate between those of Z-19 and Z-17 at 1000 hours, which indicates that a long life could have been expected.

The single drum unit, Z-21, was placed on electrolysis test to provide reference data for the larger eight-drum unit, Z-24. Both electrolyzers used a new electrode-grid style, the basic version of which, K-14, is shown in Fig. 4-4. A high conductivity, heavy duty mesh of Au/5% Pd ally made from expanded 0.025 cm thick foil is used to distribute the current uniformly over the surface of the electrode. The electrode surface consists of a base layer of electroplated platinum overlaid with platinum paste. In the K-13 version, the grid lead wires are welded to the centers of the grids. In the K-16 version, each grid is furnace brazed in seven spots to the base platinum plate of the electrode before application of the platinum paste. (See styles K-9 and K-12 for the braze pattern.) Both electrolyzers incorporate auxiliary reference electrodes as described in Section 5, below.

The one-drum unit, Z-21, was electrolyzed to failure which occurred after about 1400 hours at 100 mA/cm^2. Subsequent examination revealed all the standard degradation processes—loss of platinum paste, detachment of internal grids, and blackening and crumbling of electrolyte leading to the fracture of the disks. The early failure of unit Z-21 is not completely understood in view of the substantially longer life that has been obtained from the eight-drum electrolyzer, Z-24, which is still operating satisfactorily after more than 2000 hours. Part of the difference may be ascribed to the shock of an unscheduled power failure experienced by Z-21. The cell potentials were generally higher after resumption of electrolysis. The cell potentials of Z-24 also

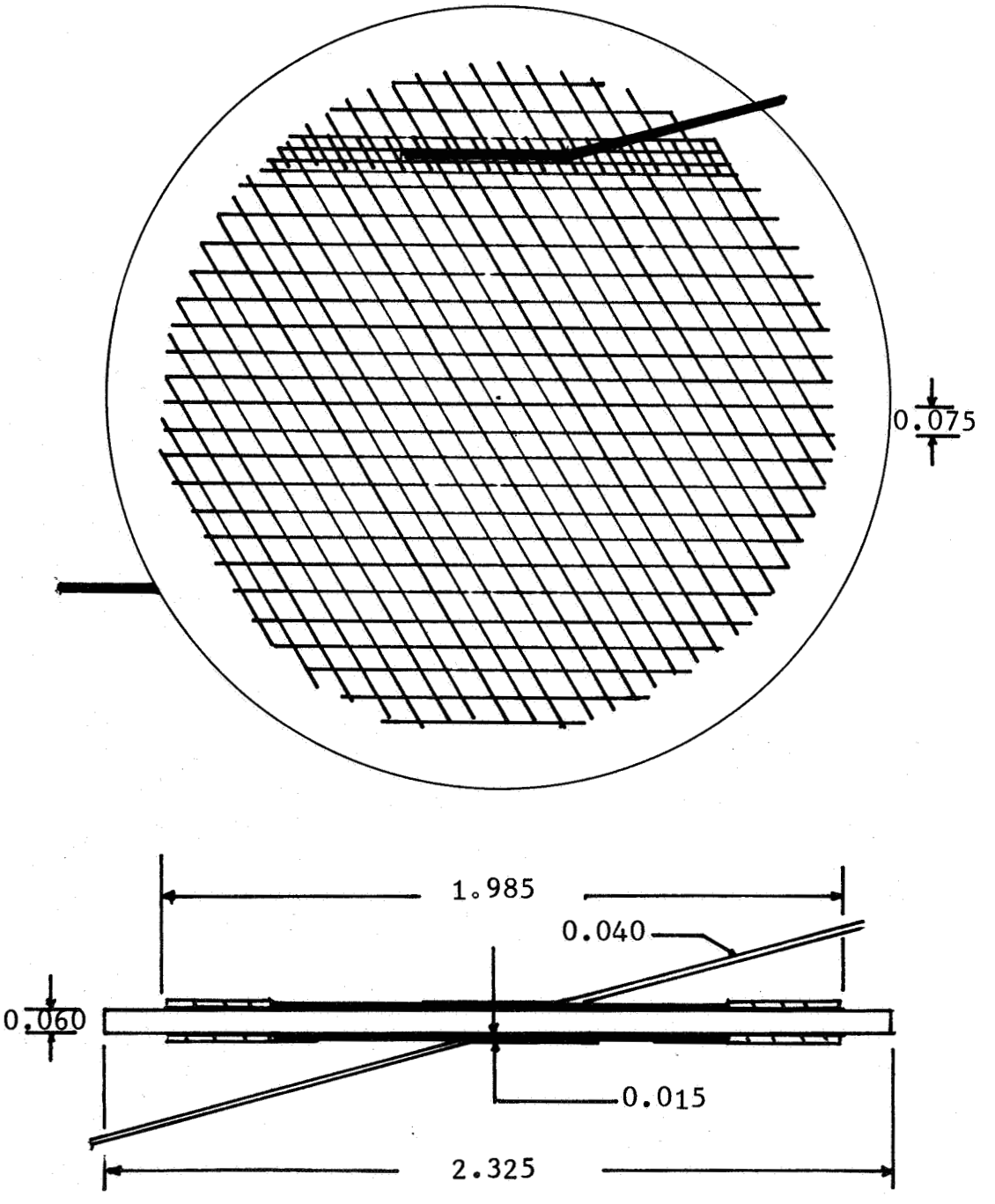

Fig. 4-4 Cell with Grid Style K-14
(Twice Actual Size, Dimensions
in Inches)

rose following the planned interruption in electrolysis for hydrogen tank changeover. Comparison of the effectiveness of the heavy gold alloy grid with the thin platinum styles previously employed cannot be made until the life-history of the eight-drum unit, Z-24, is complete. Some indication of the operating difference between the K-16 modification (grid gold brazed to platinum plate electrode) and the K-13 and K-14 versions (platinum pasted on, only) is given by the small but uniformly higher cell potentials exhibited by the K-16 gridded disks after 2000 hours of electrolysis.

The single-drum electrolyzer, Z-23, was provided with the all platinum grid style, K-19 (shown in Fig. 4-3). This style is a modification of the original K-1A style (see Fig. 4-1) where the 0.5 mm diameter wire circle, distributing the current from the lead to the mesh, has been removed from the perimeter and placed inside the electrode area to include equal areas of electrode surface both inside and outside the distribution circle. (The special wiring and operational features of this electrolyzer are described in Section 5.) Since this unit is being controlled at constant voltage, no direct comparison can be made to other electrode-grid styles in terms of cell potentials for a given time and current density. In addition, this unit has been subjected to more severe operating conditions than previous electrolyzers in terms of high CO_2 to CO conversion ratio and initial higher current density. The actual cell driving potential for Z-23, at the drum leads, is of the order of 1.7 volts. Some deterioration of electrode quality has occurred as evidenced by the decline in current density (to as low as 80 mA/cm^2 for one of the cells) after 1100 hours of operation. The life-time to failure of this unit, which can only be determined by continued electrolysis, should serve as a useful measure of the contribution of high cell voltage to electrode degradation, in general.

Section 5

OPERATION OF TEST ELECTROLYZERS

5.1 ONE-MAN (127-A) ELECTROLYZER

Units Z-10, Z-11, and Z-12 comprising the one-man electrolyzer were described in detail in the Second Annual Report (Ref. 2) including their 250-hour operational test. These units were continued in operation beyond 250 hours until serious anomalies required ending their operation.

Unit Z-10 had begun to show an increasing trend of CO_2 leakage into the oxygen envelope at 209 hours. During the occurrence of this first increase of leakage from 2.2 to 5.6%, the total applied voltage to the unit remained essentially constant (24.7 to 24.8 volts). At 258 hours, units Z-10 and Z-11 were electrically turned off to refill the humidifiers. When current to unit Z-10 was turned back up to 3.5 A (175 mA/cm^2), the applied voltage had risen to 25.7 volts from 24.7 volts. All of this rise in voltage was concentrated in the bottom cell of drum F-182, which correlates with the results found on later examination of the unit. At 264 hours, the leakage abruptly changed from 5.9 to 49.7% and the unit was turned off.

Unit Z-11 had a slowly increasing trend of CO_2 leakage throughout its life starting at 5% and reaching a level of 13.5% at 250 hours. The initial higher rate was traceable to the higher porosity of the relatively thin 0.045 inch (0.114 cm) electrolyte disks used in this unit. The increasing leak rate in this case may have been due primarily to the opening up of pores with time. Initially a sharp rise in voltage from 19.8 to 22.1 volts occurred between 21 and 23 hours of operation. A gradual rise of applied voltage during the next 120 hours was noted. This rise was reversed by maintaining the CO_2 gas flow constant and lowering the current density from 175 to 50 mA/cm^2. After six hours operation at 50 mA/cm^2, the current was raised back to 175 mA/cm^2. The applied voltage dropped down over a period of a day and remained constant at 22 to 23 volts for the next 400 hours. Shortly before the final shutdown, a gradual rise of voltage in the two cells of drum F-191 and the top cell of drum F-190 was noted. The other cells remained approximately constant over this period. The CO_2 leakage increased at the same very gradual rate until 560 hours, when a drastic increase to 31% indicated a failure and the test was stopped.

Unit Z-12 leaked almost negligibly for its first 100 hours, averaging 0.5%. Large individual cell voltage fluctuations were noted during that period. Cell voltages varied from 1.66 to 2.63 volts, with only three cells having voltages below 2 volts. At 110 hours, the rate abruptly changed to over 35%, which continued until the shutdown at 257 hours when the leakage rate had reach 40.5%.

The units were then dismantled for examination. Drums F-182 and F-184 in unit Z-10 had longitudinal cracks through the drum body, apparently originating at the stress concentrating point where the wire passes through the drum wall. In addition, the fracture appeared to have propagated from the drum body, radially across one electrolyte disk in each case. There was local discoloration on the oxygen side of the cracks, suggesting a CO flame from the leaking gas. Microscopic examination of the fracture surfaces indicated a probable origin of fracture along the wire hole, at a point where enlarged, darkened grains in the zirconia body appear. Causes can only be speculated on, but may include initial irregularity in crystal structure, thermal stress because of I^2R heating of the electrical lead wires, or electrolysis of the body material because of the voltage difference between the two lead wires. These two failed drums were separated by an intact drum, hence the failures may have been independent.

Unit Z-11 had four failed drums, with cracks similar to those in unit Z-10, except that the cracks were at gas tube holes in the drum bodies. Drums F-178, F-179, and F-181 were adjacent in the lower half of the stack, with substantial flame marking on surrounding surfaces. This suggests a drum-to-drum failure propagation, with the initial crack and CO flame causing the overheating and cracking of the drum above or below. Drum F-173, at the top of the stack, cracked at an area where a number of crystal imperfection pits in the drum surface induced local stress concentration. An additional crack in F-173 appeared at the gas tube lying directly above the failures in the lower half of the stack, suggesting it may have been flame induced.

Unit Z-12 displayed four cracked drums—F-188, F-189, F-190, and F-191—at the bottom of the stack. Again, the cracks were at the wire holes, with evidence of local discoloration caused by a CO flame with the same kind of fracture origin discussed above for unit Z-11. It is clear that the failures observed are progressive in nature, occurring only after

operation with high current density and high rates of oxygen transfer through the cells. The hanging of the drums from the gas tubes and lead wires adds local components of torsion and tensile stress which combine with the hoop stress in the drum body due to thermal expansion. Combination of those stresses with grain growth and electrochemical effects resulted in eventual failure.

The three-inch diameter steel low carbon CO disproportionator operating on the $CO-CO_2$ streams from units Z-10, Z-11, and Z-12 had a heated furnace 60 cm long which could be moved along the length of the reactor. The temperature was held at 552 $\pm$ 8°C for most of the run. The furnace was moved along a 60 cm length of the pipe in both directions. Atthe end of the run (550 hours for one unit, 257 hours for all three), the reactor was cooled and the carbon was removed. A total of 701 grams of loose, finely divided carbon had accumulated.

5.2 TWO-DRUM UNITS Z-13 AND Z-14

Two electrolyzers with two drums each were assembled in order to make preliminary tests of some new grid and tubing configurations.

Unit Z-13 used the gold alloy cross plus concentric circle grids. Entrance tubing in the drums included a 90-degree elbow inside the drum, as shown in Fig. 5-1. Improved current and gas flow distribution were the aims of these changes. The cells were wired in series. Gold-palladium wire was used for leads rather than the platinum previously used. Connecting sleeves of gold alloy were arranged so that tubing stubs on the drums and on the manifolds could be joined by torch brazing.

Oxygen electrolysis conditioning was carried on for 69 hours in forward and reverse directions with currents to 4 A. CO_2 electrolysis was then started with a 4.5 hour buildup to full power. After 64 hours the oxygen yield abruptly declined to 58% and a short circuit was detected at the upper grid of the lower drum. The unit was turned off and cooled to room temperature for examination. The upper drum, F-207, had sagged and shorted across the connections to the upper grid on drum F-206 below it. This was attributed to the long span of metal tubing connecting the drum to the manifolds, as well as the gold alloy connecting wires which lacked the stiffness of platinum wire. A ceramic spacer was placed

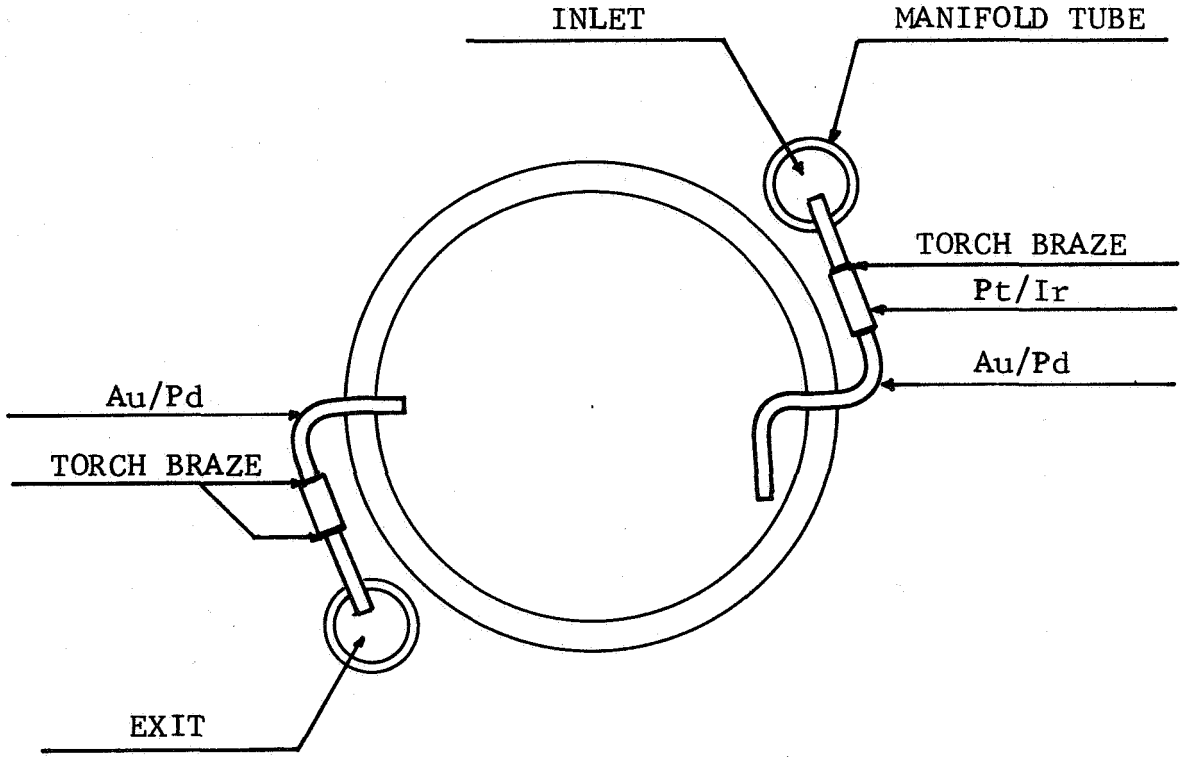

Fig. 5-1 Module Z-13 Gas Port Connections

between the drums and the unit was re-assembled in its envelope. Operating time was counted from the resumption of full power at operating temperature. After correction of the short circuit, the voltage rise at 4 A for the next 200 hours was 2.46 to 2.73 V and 2.29 to 2.55 V for the top and bottom cells of the upper drum, respectively; 2.34 to 2.54 V and 2.28 to 2.48 V for the top and bottom cells of the lower drum, respectively.

The run continued for 350 hours with a somewhat declining oxygen efficiency (below 90% for the last 72 hours) but a very low leakage rate. The CO_2 to O_2 leakage did not exceed 0.33% until the final breakdown at 374 hours. Just before that breakdown, the oxygen efficiency had dropped below 80% and the leak rate rose from 0.1 to 0.3%. Also, the top disk of the upper drum shorted out.

On dismantling the unit, the upper and lower drums were cracked. The upper drum, F-207, cracked at a thin section of its periphery which was further stressed because of some pits from crystalline defects in the zirconia material. It is probable that this crack occurred first and that heating from the CO flame at that point induced the adjacent drum to crack. The electrolyte disks did not crack, but were thoroughly degraded in patterns lying under the gold wires. The degradation had perforated the electrolyte on the upper disks of both the upper and lower drums. The electrical data tends to indicate that the perforation occurred before the drum cracking. In spite of this drastic deterioration at 374 hours operation, the unit performed well for greater than 350 hours.

Unit Z-14 used grids incorporating high-conductivity gold alloy wire described in sub-section 4.4, above. Gas tubing and manifolding were of the same type used in the previous one-man electrolyzer. The cells were wired so that the two negative grids on the inside of each drum were in parallel and also the two positive grids on the outside but the two drums were in series. Thus to carry the desired 4 A to each cell, the major current leads entering the electrolyzer envelope carried 8 A. The grids were the same for all four cells. Top and bottom disks were 0.069 and 0.073 inch thick for drum F-203 and 0.070 and 0.078 inch for drum F-205.

The unit was pre-conditioned with 120 hours of oxygen electrolysis using currents of 2 to 8 A in both drum-to-envelope and envelope-to-drum directions. CO_2 electrolysis then commenced with a conservative buildup to full power covering

25 hours. Operation at 4 A per cell then continued for 331 hours. For that period, the oxygen yield was 80 to 90%. CO_2 leakage in the oxygen stream remained below 1% for 168 hours and slowly increased to 2.3% at 311 hours.

The voltage of the top drum remained practically constant for the first 300 hours at 2.68 to 2.85 volts. At 329 hours the voltage rose abruptly to 3.59 volts from a previous level of 2.85 volts. The CO_2 leakage also abruptly rose to 89% and the test was terminated. In contrast, the initial applied voltage to the lower drum was 2.11 volts. At 90 hours, the voltage was 2.55 volts and rose gradually to 2.69 volts at 329 hours.

On dismantling the unit, the upper drum (F-203) was found to have cracked, with the crack propagating across both faces of the electrolyte disks. The lower drum (F-205) remained gas-tight. Careful examination suggested that the fracture in the upper drum probably started at a lump of excess sealing gold in the corner between the drum and the disk, located where it would induce tension on expansion. The abrupt change in voltage at 329 hours is associated with this fracture of the electrolyte. Both upper and lower drums showed substantial detachment of the current grids from the electrolyte faces. The inner grids (CO_2 side) were fully detached in the upper drum and three-fourths detached in the lower drum. There was a marked degradation of electrolyte under the gold alloy cross of the grids on both inner and outer surfaces. Differential expansion of gold and zirconia may have induced the detachment. The electrolyte degradation mechanism was discussed in Section 4, above.

5.3 SIX-DRUM UNIT Z-17

The construction details of a typical drum of unit Z-17 are shown in Fig. 5-2. The gas port tubulation connection angle and method of mounting in a horizontal furnace used in this unit reflect an intermediate stage in the changeover from the old vertical to the new horizontal testing geometry. The drums for this module had already been brazed using the old opposed angle on the two gas port tubulations of each drum. The accommodation to horizontal operating position is shown in Fig. 5-3. The torch brazing method showed its versatility in this unit when one drum was damaged in the assembly. Its tubes were sawed off and a new drum was brazed

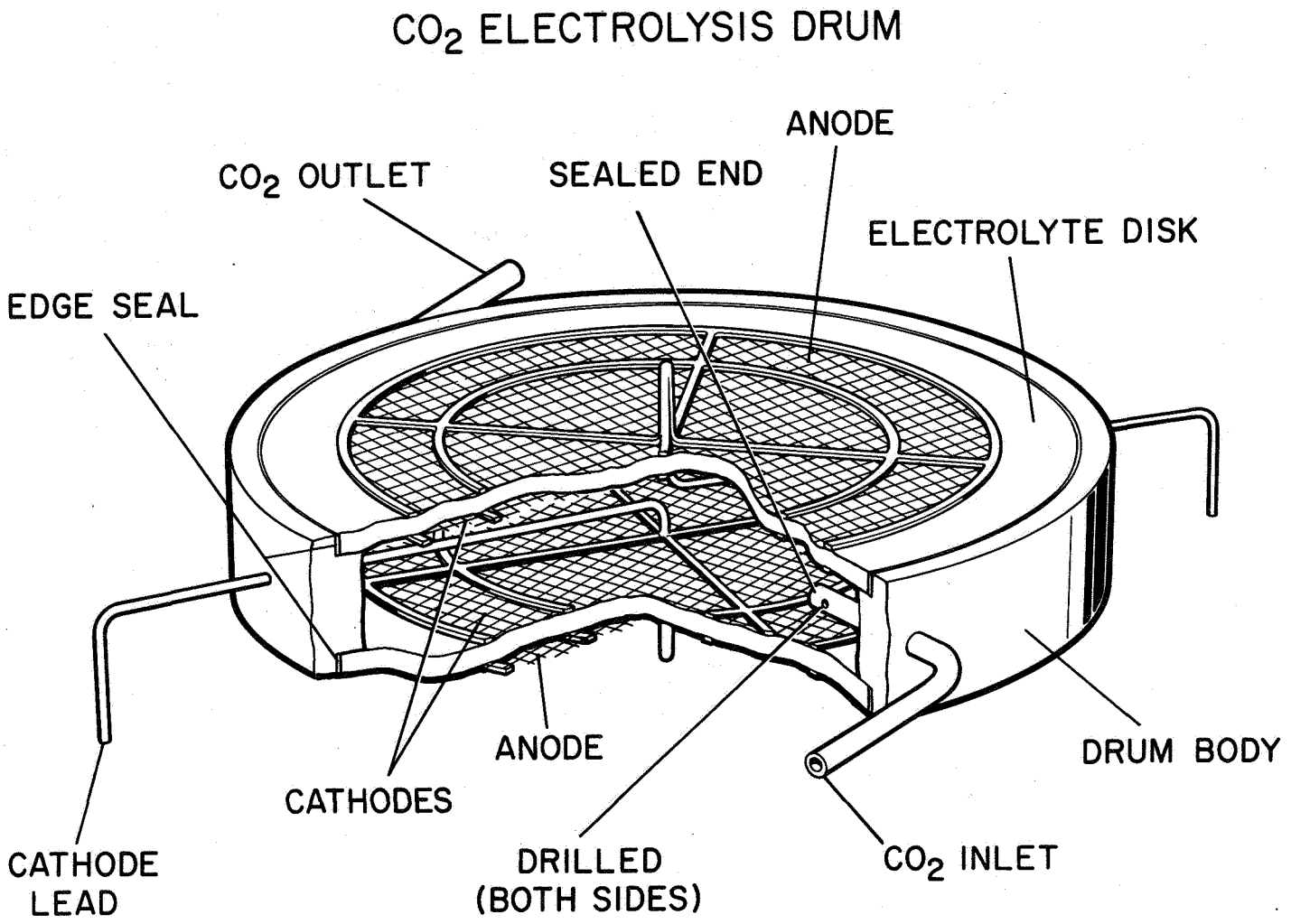

Fig. 5-2 Details of Drum Construction for Unit Z-17

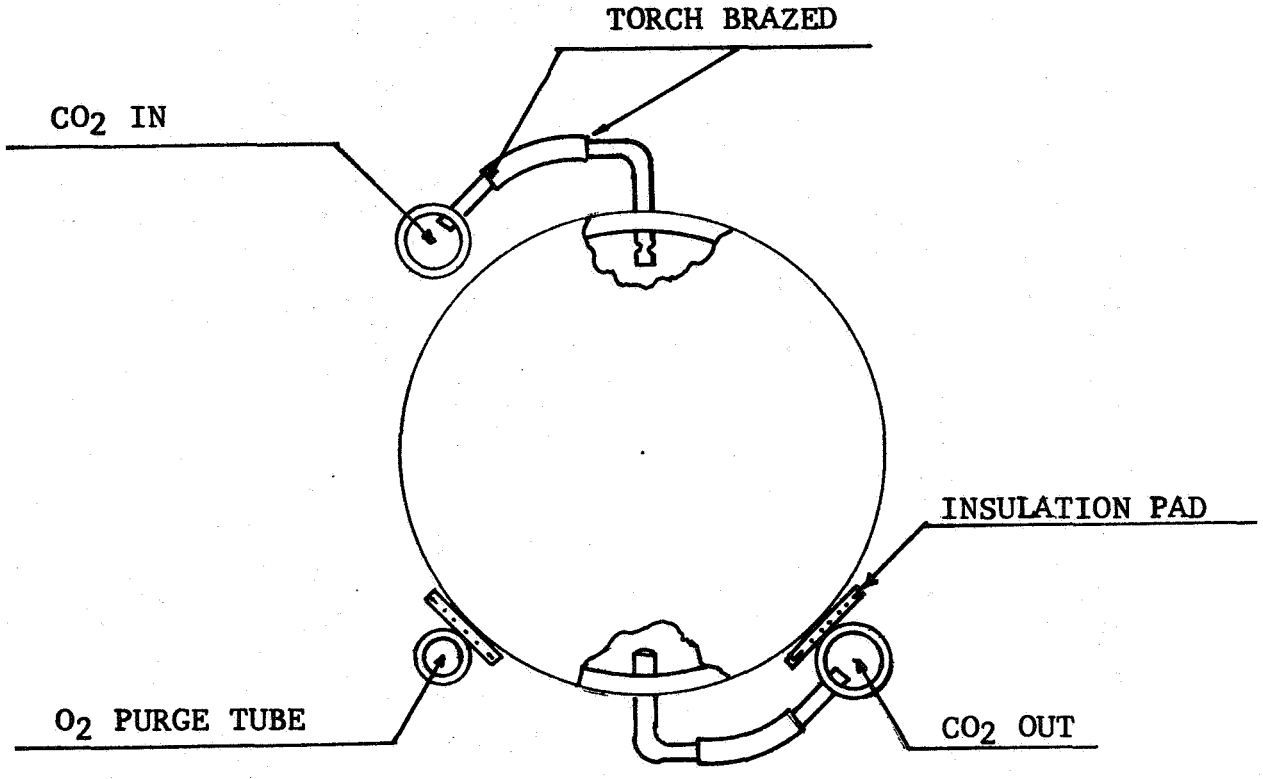

Fig. 5-3 Torch-Brazed Manifold Connections and Method of Supporting Drums in Horizontal Furnace for Unit Z-17

in as a replacement, a repair technique which was not previously available in the sealing process. The complete assembly tested at over four minutes in the $\Delta t/\Delta p$ leak test (dry gauge system) previously described (Section 7 of Ref. 2).

The drums were basically the same 20 cm^2 disks and edge seal design described in the Second Annual Report (Ref. 2) with modifications to the electrical grid and gas inlet tubes. The grid with increased current carrying capacity and the two-port inlet nozzle for better flow distribution are described in sub-sections 4.3 and 3.5. Drum bodies were made from calcia-stabilized zirconia and the electrolyte disks were of $(ZrO_2)_{0.93}(Sc_2O_3)_{0.07}$.

A horizontal furnace was provided to operate the electrolyzer in a horizontal position. One advantage is that the manifold tubes can be arranged to carry the weight of the drums, as shown in Fig. 5-3, thus avoiding strain on the connecting tubes. A supporting disk of Lava A was placed at the end of the drum stack to space the manifold tubes and carry the weight.

Wiring connections between drums were also changed to minimize leakage currents. There has been some concern that the somewhat conductive calcia-zirconia drum bodies tend to carry small currents between the wire leads which pass through the drum walls and adjacent disk edges. With the previous wiring arrangement, each drum had one area in which a two-volt potential was separated by 0.2 cm of calcia-zirconia. The revised wiring, shown in Fig. 5-4, results in a maximum of one-volt difference at any point. The "upper" cells are in series with each other and the "lower" cells are in series in a completely separate circuit. The two groups of cells are then connected to two separate power supplies.

Unit Z-17 was first pre-treated with oxygen at one and two amperes per cell and with carbon dioxide at one ampere per cell. CO_2 electrolysis was then initiated at two amperes per cell (100 mA/cm^2) at a temperature of 870°C. The nominal CO_2 flow rate was 730 ml/min during the electrolysis at two amperes per cell. The twelve-cell electrolyzer was operated continuously under these conditions of CO_2 electrolysis for 86 days (2050 hours). Subsequent operation under similar conditions continued to 115 days (2700 hours).

The following operating parameters were generally measured on a daily basis during the 115 days:

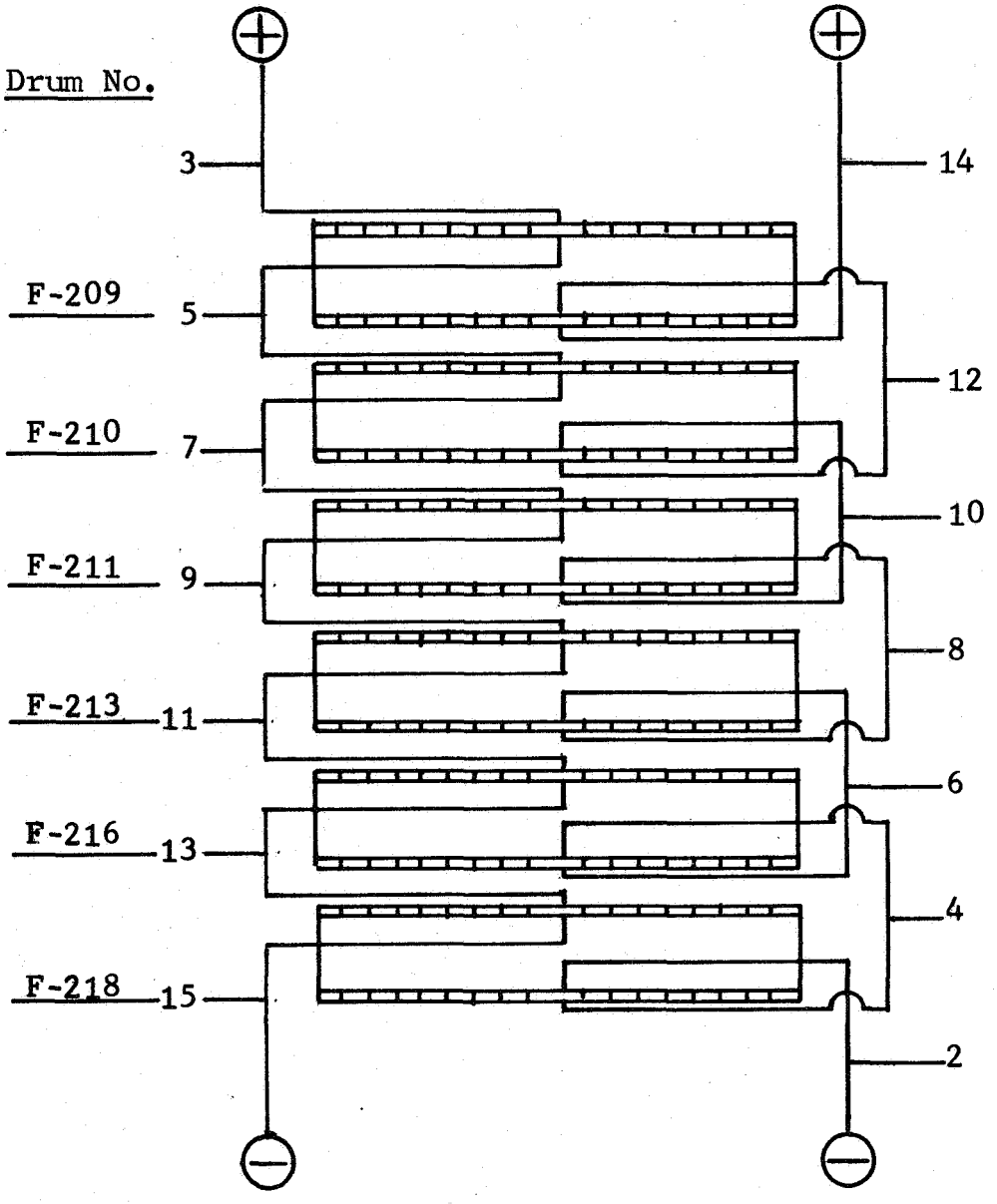

Numbers 2 to 15 - Voltage probes
⊖, ⊕ - leads to power supply

Fig. 5-4 Wiring Diagram for Unit Z-17

Electrolyzer envelope temperature

Carbon dioxide-water flow rate

Twelve single cell voltages

Total oxygen yield

Carbon dioxide content of the oxygen stream

Carbon monoxide content of the exit carbon dioxide-carbon monoxide stream

Current to each bank of six cells

Complete data are listed in Table 5-1.

The total applied voltage for the twelve cells, the percent oxygen yield (faradaic current efficiency), and the CO_2 content in the oxygen stream are shown in Fig. 5-5 as a function of the number of days of operation for the first 101 days. The CO_2 to CO conversion rate per pass measured during this period was 20 to 27 percent. As shown in Fig. 5-5, there was a relatively rapid decline in the total applied voltage during the first few days of operation after which a gradual rise in voltage occurred. The initial decrease in voltage can be ascribed predominately to improvement in the electrode and grid contacts. Further continuous operation leads to a gradual loss of electrode and grid contacts on the cathode (reducing) side and irreversible changes in the high current density portions of the electrolyte because of non-uniform distribution of current on the electrodes. The result is an increase in the total cell resistance which manifests itself by an increase in the applied voltage (at constant current). The periodic fluctuations in the applied voltage seen in Fig. 5-5 result from changes in the resistance of the twelve cells (at constant current) due to cycling of the furnace temperature. The variation of the uncorrected oxygen yield between 98 and 104% in Fig. 5-5 is due to fluctuation of the oxygen volume flow rate with fluctuation of the temperature in the test room. A correction in the oxygen flow rate must also be made for the partial saturation of the oxygen stream with water at the soap bubble meter.

Typical variations in the single-cell voltage values, V_{CO_2}, for the twelve cells is shown in Table 5-2 for the eighth day of CO_2 electrolysis. Included in the table are the single

Table 5-1

OPERATING DATA FOR SIX-DRUM ELECTROLYZER Z-17

Date	Day	Total Hours	CELL VOLTAGES												O_2 Yield (%)	CO_2 in O_2 (%)
			Upper Cell, Drum No.						Lower Cell, Drum No.							
			209	210	211	213	216	218	209	210	211	213	216	218		
6/29	Break-		1.68	1.58	1.58	1.58	1.59	1.66	1.65	1.58	1.57	1.58	1.58	1.66	100	0.14
6/29			1.65	1.58	1.58	1.57	1.61	1.64	1.54	1.57	1.52	1.55	1.56	1.63	-	-
6/29			1.66	1.58	1.59	1.57	1.61	1.64	1.52	1.57	1.56	1.56	1.56	1.63	102	0.20
6/30	in		1.57	1.36	1.75	1.44	1.80	1.43	1.66	1.43	1.36	1.37	1.48	1.48	95.5	0.26
6/30			1.56	1.39	1.71	1.48	1.41	1.51	1.68	1.47	1.38	1.43	1.49	1.48	99	0.27
7/1	Period		1.62	1.51	1.51	1.40	1.52	1.55	1.80	1.54	1.46	1.50	1.55	1.52	98	0.34
7/1	1	0	2.16	1.88	1.73	1.97	1.93	1.99	2.36	1.93	1.78	1.85	1.98	1.98	104.5	0.21
7/2	2	18	2.28	2.15	2.04	2.16	2.15	2.22	2.35	2.17	2.10	2.17	2.17	2.21	99.5	0.12
7/2		24	2.23	1.87	1.55	1.98	2.15	1.77	2.31	1.98	1.58	1.64	2.10	2.02	103.5	0.11
7/6	6	113	1.87	1.89	1.61	1.70	1.70	1.80	2.20	1.64	1.71	1.87	1.72	1.96	98	0.14
7/7	7	140	1.88	1.90	1.60	1.64	1.95	1.78	2.38	1.79	1.63	1.71	1.73	1.80	99	0.16
7/7		144	1.88	1.92	1.61	1.67	1.70	1.80	2.30	1.82	1.64	1.73	1.73	1.81	101	0.22
7/8	8	163	1.93	1.77	1.69	1.73	1.76	1.85	1.92	1.89	1.71	1.88	1.78	1.84	99.5	0.22
7/9	9	185	1.86	1.93	1.63	1.80	1.97	1.78	1.98	1.85	1.64	1.72	1.71	1.78	99	-
7/9		190	1.71	1.55	1.51	1.65	1.55	1.64	1.92	1.74	1.54	1.60	1.58	1.65	100	0.22
7/10	10	209	1.86	1.66	1.68	1.75	1.62	1.73	1.89	1.83	1.69	1.80	1.70	1.74	101.5	0.19
7/13	13	284	1.72	1.77	1.46	1.56	1.57	1.67	1.85	1.64	1.56	1.68	1.59	1.66	102	0.20
7/14	14	308	1.77	1.69	1.56	1.60	1.67	1.74	1.85	1.81	1.70	1.60	1.64	1.71	103.5	0.21
7/15	15	330	1.85	1.85	1.74	1.58	1.57	1.64	1.98	1.65	1.56	1.86	1.63	1.78	102.5	0.20
7/16	16	353	1.86	1.68	1.56	1.70	1.63	1.72	1.89	1.76	1.71	1.56	1.59	1.92	101.5	0.20
7/17	17	377	1.79	1.78	1.69	1.62	1.72	1.80	1.98	1.63	1.56	1.62	1.74	1.71	101.5	0.20
7/20	20	449	1.83	1.71	1.58	1.78	1.64	1.73	1.96	1.64	1.70	1.59	1.65	1.71	102.5	0.21
7/21	21	476	2.01	1.91	1.46	1.56	1.55	1.96	1.82	1.71	1.46	1.47	1.52	1.86	103	0.20
7/22	22	502	1.77	1.69	1.60	1.55	1.64	1.73	1.93	1.71	1.57	1.61	1.61	1.74	103.5	0.22
7/23	23	521	1.82	1.76	1.68	1.67	1.72	1.79	2.08	1.78	1.63	1.62	1.65	1.94	102	0.25
7/24	24	546	1.87	1.75	1.60	1.60	1.66	1.93	1.87	1.70	1.69	1.68	1.71	1.72	102.5	0.28
7/27	27	617	1.99	1.80	1.70	1.63	1.67	1.73	2.17	1.77	1.58	1.58	1.65	1.71	101.5	0.23
7/28	28	646	1.80	1.73	1.61	1.69	1.70	1.78	1.87	1.68	1.64	1.65	1.71	1.74	102	0.23
7/29	29	665	1.91	1.81	1.76	1.70	1.76	1.90	1.94	1.71	1.75	1.70	1.76	1.82	101.5	0.27

continued

Table 5-1, OPERATING DATA FOR SIX-DRUM ELECTROLYZER Z-17 (continued)

Date	Day	Total Hours	CELL VOLTAGES												O_2 Yield (%)	CO_2 in O_2 (%)
			Upper Cell, Drum No.						Lower Cell, Drum No.							
			209	210	211	213	216	218	209	210	211	213	216	218		
7/30	30	697	1.82	1.71	1.73	1.70	1.77	1.93	1.71	1.78	1.71	1.68	1.77	1.87	104	0.26
7/31	31	713	1.97	1.64	1.56	1.63	1.86	2.00	1.85	1.61	1.56	1.75	1.85	1.99	101.5	0.23
8/3	34	785	1.90	1.78	1.70	1.66	1.83	1.82	2.00	1.74	1.67	1.64	1.68	1.82	102	0.25
8/4	35	812	2.04	1.88	1.58	1.73	1.70	1.75	2.01	1.86	1.54	1.62	1.80	1.72	103.5	0.23
8/5	36	838	1.92	1.80	1.78	1.72	1.59	1.92	1.90	1.75	1.76	1.75	1.68	1.90	104	0.27
8/6	37	863	1.85	1.65	1.63	1.63	1.66	1.75	1.95	1.63	1.59	1.62	1.66	1.74	105	0.26
8/7	38	882	2.02	1.85	1.81	1.56	1.65	1.91	2.08	1.82	1.79	1.56	1.60	1.90	102.5	0.32
8/10	41	953	2.04	1.89	1.76	1.76	1.86	1.88	2.10	1.85	1.74	1.81	1.79	1.85	103	0.28
8/11	42	980	2.09	1.92	1.55	1.72	1.63	1.68	2.13	1.90	1.51	1.77	1.57	1.67	105	0.25
8/12	43	1009	1.88	1.76	1.67	1.66	1.65	1.78	1.91	1.73	1.60	1.60	1.71	1.78	105.5	0.26
8/13	44	1026	2.11	1.94	1.83	1.86	1.75	2.01	2.13	1.92	1.79	1.90	1.84	2.01	101.5	0.25
8/14	45	1049	2.00	1.82	1.78	1.73	1.91	1.86	2.10	1.80	1.75	1.83	1.75	1.83	100.5	0.33
8/17	48	1121	1.97	1.95	1.82	1.71	1.73	1.80	2.00	1.64	1.70	1.61	1.67	1.69	100	0.31
8/18	49	1150	1.92	1.82	1.80	1.65	1.68	1.93	1.93	1.78	1.77	1.65	1.62	1.84	103	0.32
8/19	50	1172	1.97	1.77	1.67	1.73	1.77	1.75	2.00	1.75	1.61	1.76	1.74	1.78	101	0.38
8/20	51	1196	2.06	1.90	1.80	1.62	1.92	1.85	2.12	1.85	1.77	1.55	1.82	1.96	103	0.28
8/21	52	1218	2.00	1.80	1.84	1.72	1.72	1.89	2.05	1.78	1.80	1.68	1.75	1.84	102	0.30
8/24	55	1289	2.10	1.85	1.76	1.91	1.79	1.98	2.12	1.82	1.73	1.73	1.78	1.88	100	0.27
8/25	56	1313	2.00	1.86	1.79	1.70	1.87	1.85	2.05	1.83	1.77	1.81	1.80	1.91	-	0.30
8/26	57	1339	2.12	1.83	1.81	1.75	1.75	1.93	2.11	1.80	1.77	1.73	1.80	1.85	99	0.32
8/27	58	1362	1.97	1.95	1.80	1.65	1.75	1.82	2.05	1.90	1.78	1.55	1.66	1.70	100	0.30
8/28	59	1385	2.05	1.81	1.80	1.80	1.90	2.00	2.10	1.78	1.74	1.70	1.75	1.84	101.5	0.31
8/31	62	1464	1.98	1.95	1.65	1.70	1.72	1.86	2.02	1.95	1.67	1.72	1.68	1.92	101.5	0.31
9/1	63	1481	2.10	1.80	1.81	1.77	1.81	1.81	2.10	1.77	1.79	1.85	1.80	1.73	100	0.32
9/2	64	1505	2.01	1.85	1.82	1.78	1.81	1.99	2.06	1.82	1.77	1.71	1.84	1.84	99.7	0.31
9/3	65	1530	2.15	1.90	1.80	1.84	1.74	1.87	2.08	1.85	1.79	1.82	1.73	1.90	100.6	0.32
9/4	66	1554	1.99	1.85	1.87	1.72	1.78	1.99	2.08	1.83	1.80	1.72	1.80	1.91	100.6	0.32
9/8	70	1649	2.05	1.91	1.89	1.82	1.80	2.00	2.11	1.88	1.81	1.83	1.80	-	101	0.36
9/9	71	1673	2.11	1.85	1.82	1.77	1.80	2.00	2.12	1.82	1.82	1.74	1.60	-	100	0.37
9/10	72	1697	2.00	1.93	1.87	1.87	1.75	1.98	2.06	1.90	1.78	1.87	1.75	-	98.5	0.38
9/11	73	1722	2.18	1.82	1.85	1.72	1.76	1.99	2.14	1.81	1.82	1.72	1.78	-	101	0.36
9/14	76	1793	2.06	2.02	1.91	1.77	1.81	2.00	2.09	1.99	1.80	1.77	1.81	-	99	0.39

continued

Table 5-1, OPERATING DATA FOR SIX-DRUM ELECTROLYZER Z-17 (continued)

Date	Day	Total Hours	CELL VOLTAGES												O_2 Yield (%)	CO_2 in O_2 (%)
			Upper Cell, Drum No.						Lower Cell, Drum No.							
			209	210	211	213	216	218	209	210	211	213	216	218		
9/15	77	1817	2.13	1.93	1.86	1.85	1.87	1.83	2.11	1.90	1.80	1.85	1.87	-	100	0.39
9/16	78	1842	2.10	1.91	1.91	1.90	1.88	2.01	2.16	1.92	1.83	1.84	1.90	-	100	0.37
9/17	79	1865	2.17	1.97	1.89	1.78	1.84	2.03	2.13	1.93	1.83	1.80	1.82	-	100	0.40
9/18	80	1889	2.09	1.94	1.89	1.77	1.82	2.20	2.10	1.92	1.81	1.73	1.79	-	99	0.43
9/21	83	1961	2.19	1.92	1.94	1.94	1.96	2.04	2.20	1.93	1.85	1.92	1.95	-	100	0.38
9/22	84	1993	2.03	1.84	1.84	1.76	1.78	2.01	2.05	1.82	1.76	1.75	1.77	-	104	0.41
9/23	85	2009	2.08	1.92	1.89	1.78	1.80	2.02	2.10	1.91	1.82	1.77	1.80	-	103.5	0.38
9/24	86	2039	1.93	1.94	1.70	1.62	1.69	1.98	1.94	1.92	1.63	1.65	1.68	-	101	0.39
9/24	86	2050	Power down													
9/29	86	2050	Power up													
9/29	87	2058	2.63	2.43	2.18	2.31	2.20	2.20	2.65	2.34	1.95	2.15	2.24	2.24	100.5	-
9/30	88	2082	2.33	2.32	1.96	1.99	1.90	2.03	2.44	2.38	1.85	1.90	1.90	2.18	99.8	0.49
10/1	89	2105	2.27	2.39	2.02	1.95	2.00	2.08	2.35	2.40	1.90	1.94	2.04	2.24	100.6	0.48
10/2	90	2129	2.44	2.20	1.96	1.91	1.90	1.98	2.48	2.35	1.88	1.89	1.91	2.20	101	0.45
10/5	93	2201	2.23	2.05	2.00	1.96	1.95	2.12	2.35	2.26	1.89	2.00	2.05	2.17	99.7	0.41
10/6	94	2225	2.27	2.17	1.93	2.05	1.85	1.96	2.36	2.25	1.83	1.86	1.88	2.16	99.7	0.45
10/7	95	2249	2.41	2.03	2.00	1.88	1.90	2.00	2.56	2.46	1.91	1.91	2.10	2.19	98	0.46
10/8	96	2273	2.22	2.10	1.95	1.90	1.89	1.99	2.33	2.26	1.84	1.93	1.88	2.09	99.7	0.46
10/9	97	2297	2.26	2.51	1.98	1.92	1.92	2.02	2.35	2.35	1.87	1.85	1.90	2.18	99.7	0.46
10/12	100	2371	2.25	2.54	1.95	1.97	1.90	2.02	2.32	2.35	1.87	1.94	1.88	2.12	98.8	0.48
10/13	101	2399	2.20	2.56	1.90	1.89	1.84	1.91	2.38	2.48	1.77	1.84	1.85	2.06	99.7	0.47
10/13	102	2422	Current off													
10/14	102	2422	Current on - 1½% H_2 in CO_2 input													
10/14	102	2422	2.75	2.65	2.28	2.38	2.25	2.26	2.77	2.81	2.05	2.24	2.32	2.49	-	-
10/15	103	2441	2.15	2.64	1.95	1.90	1.90	2.08	2.25	2.73	1.87	1.85	2.73	2.25	96.2	1.25
10/16	104	2463	2.27	2.63	2.02	1.94	1.94	2.44	2.35	2.67	1.88	1.99	2.02	1.62	94	1.20
10/19	107	2537	2.43	2.76	1.95	1.90	1.72	2.56	2.36	2.96	1.86	1.90	1.74	2.74	93	3.2
10/19	107	2537	Power down for examination - one drum removed													
10/28	107	2537	Power up													
10/29	109	2557	3.05	-	2.52	2.70	2.38	2.74	3.13	-	2.20	2.40	2.50	3.07	94	-
10/30	110	2577	2.92	-	2.13	2.18	2.07	2.68	2.59	-	2.00	2.08	2.22	2.91	94	0.97
11/2	113	2649	2.62	-	2.00	2.47	2.38	2.66	2.60	-	1.90	2.27	2.47	2.92	89	2.18
11/3	114	2673	2.48	-	2.20	2.47	2.45	2.63	2.53	-	2.08	2.34	2.56	3.43	90	2.94
11/4	115	2699	2.59	-	2.06	2.53	2.35	2.80	Broken circuit						63	4.03
11/4	115	2700	Electrolysis terminated													

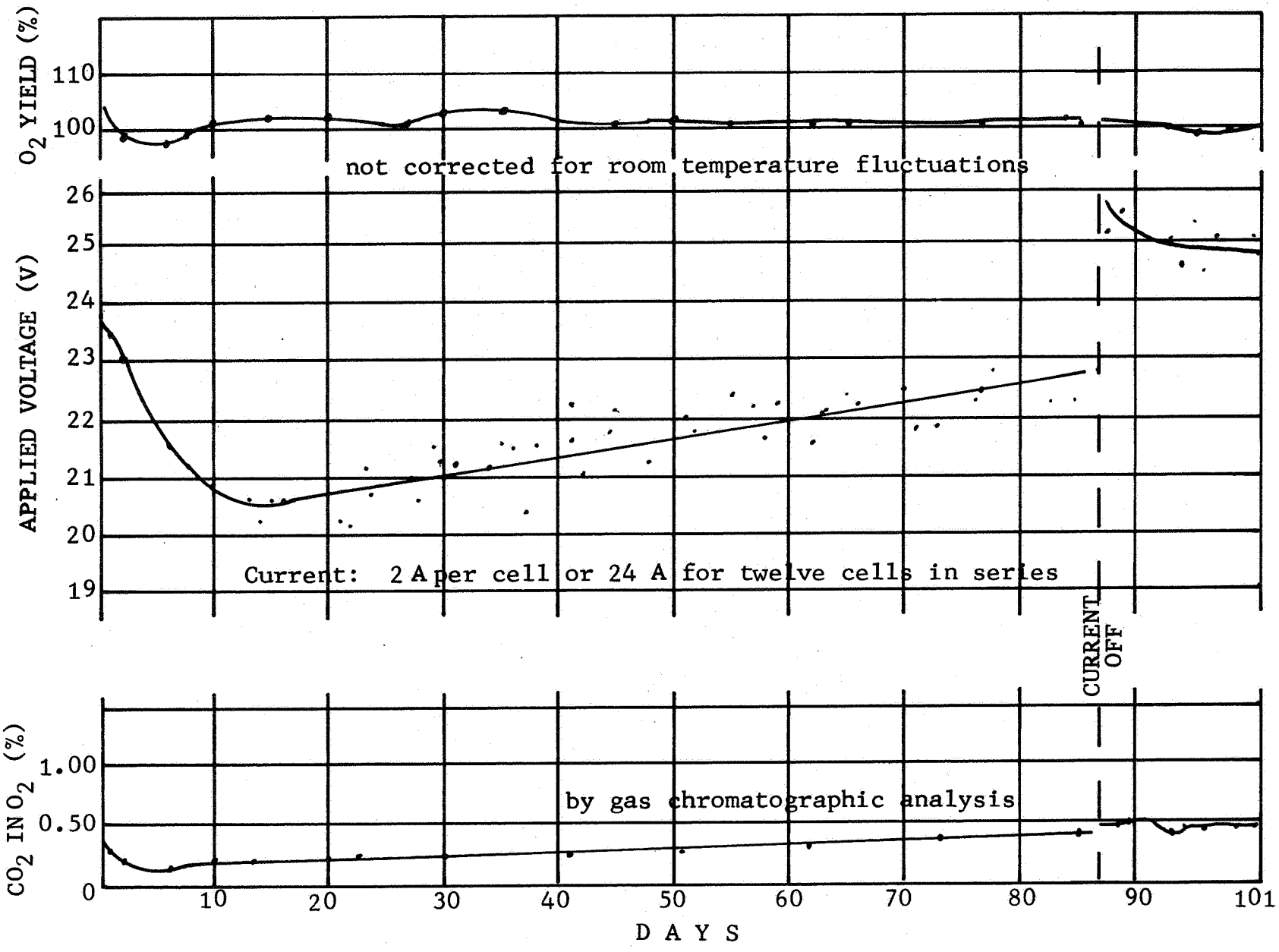

Fig. 5-5 Performance of Twelve-Cell Electrolyzer Z-17
Operating at 100 mA/cm^2 and 875^{o}C

Table 5-2

TYPICAL SINGLE CELL VOLTAGES FOR ELECTROLYZER Z-17

PROCESS	APPLIED VOLTAGE (V)[a]					
	Drum Numbers					
	F-209	F-210	F-211	F-213	F-216	F-218
	TOP CELLS					
CO_2 electrolysis	1.93	1.77	1.69	1.73	1.76	1.85
O_2 transfer	0.56	0.39	0.37	0.37	0.40	0.55
$\Delta V_{CO_2} = V_{CO_2} - V_{O_2}$[c]	1.37	1.38	1.32	1.36	1.36	1.30
$V_p = \Delta V_{CO_2} - \bar{E}$[d]	0.53	0.54	0.48	0.52	0.52	0.46
	BOTTOM CELLS					
CO_2 electrolysis[b]	1.92	1.89	1.71	1.88	1.78	1.84
O_2 transfer	0.53	0.38	0.34	0.38	0.38	0.55
$\Delta V_{CO_2} = V_{CO_2} - V_{O_2}$[c]	1.39	1.51	1.37	1.50	1.40	1.29
$V_p = \Delta V_{CO_2} - \bar{E}$[d]	0.55	0.67	0.53	0.66	0.56	0.45

[a]Not corrected for IR drop in the current leads of 0.1 volt per bank of six cells (cells in drums F-209 and F-218)

[b]Voltage values from eighth day of 115-day test (see Table 5-1)

[c]ΔV_{CO_2} measured is the sum of the theoretical CO_2 dissociation voltage and the polarization voltage term (see Eq. 5-4)

[d]$\bar{E}$ = 0.84 V obtained from Eq. 5-2 with E^o = 0.95 V.

cell voltage values, V_{O_2}, for electrolytic oxygen transfer under the same conditions of current and temperature, and the difference in voltage, $V_{CO_2}-V_{O_2}$.

For electrolytic oxygen transfer, the partial pressures of oxygen at the cathode, ${}_cPO_2$, and anode, ${}_aPO_2$, are both one atmosphere. The applied voltage must then only overcome the total cell resistance, R_T, at a particular current, I. Concentration polarization and activation overvoltage for the oxygen/platinum cathode and anode (based on previous experimental evidence) are taken as zero. Therefore,

$$V_{O_2} = I R_T \qquad (5\text{-}1)$$

Contributions to the total resistance, R_T, include the resistances of the electrolyte, electrolyte-electrode contacts, grids, and inter-cell electrical leads otherwise not removed by voltage probes.

For CO_2 electrolysis, the applied voltage, V_{CO_2}, in addition to the $I R_T$ term, must include the theoretical average voltage, $\bar{E}_{CO_2}$, for the dissociation of CO_2 to CO and O_2, given by the equation

$$\bar{E} = E^o + \frac{RT}{2F\Delta n} \quad (n_i \ln p_i - n_f \ln p_f) \qquad (5\text{-}2)$$

where $\bar{E}$ is the average and E^o the standard theoretical voltage, Δn the moles of CO_2 converted to CO and n_i, p_i, n_f, p_f are the initial and final moles and pressures of CO and CO_2. The equivalent log term drops out for ${}_aPO_2 = 1$ atm. A polarization voltage term, V_p, defined as the sum of the activation overvoltage, concentration polarization voltage, and other polarization phenomena associated with the CO_2 electrode (cathode) reaction, must also be included. Therefore, the applied voltage, V_{CO_2}, is given by the equation

$$V_{CO_2} = \bar{E} + V_p + R_T I \qquad (5\text{-}3)$$

From Equations (5-1) and (5-3)

$$\Delta V_{CO_2} = V_{CO_2} - V_{O_2} = \bar{E} + V_p \qquad (5\text{-}4)$$

ΔV_{CO_2}, the experimentally obtained difference in voltage, is the sum of the CO_2 dissociation voltage, $\bar{E}$, and the polarization voltage term, V_p. R_T of the cell in Equations 5-1 and 5-3 is assumed to remain constant for both processes occurring

at the same temperature when measured at approximately the same time during the cell's operating history. An equivalent large increase in R_T was previously observed for both CO_2 electrolysis and oxygen transfer after 30 days of near perfect operation of the eight-ampere one-drum electrolyzer Z-8 (Ref 2).

The ΔV_{CO_2} values per cell in electrolyzer Z-17 are about 0.2 volt higher than in electrolyzer Z-8. This discrepancy can be ascribed to the gradual drop in contact resistance in the cells of unit Z-17 during the initial two weeks of operation and the fact that V_{CO_2} was measured during the middle of this period while V_{O_2} was measured before the start of CO_2 electrolysis.

After 2050 hours of operation, unit Z-17 was cooled down, removed from the furnace and visually examined for signs of physical degradation of the outside cells, drum walls, and seals. No signs of serious physical degradation of the cells were evident.

The electrolyzer was put back into operation under the same conditions prevailing before the shutdown. Referring to Fig. 5-5, it is apparent that the resistance of the electrolyzer increased about 10%. The process of cooling the unit to room temperature, removing from the furnace, and re-heating to operating temperature had the effect of increasing the cell resistances. The electrolyzer continued to operate satisfactorily at 100% average O_2 yield and less than 0.5% CO_2 in the oxygen output for an additional 15 days. It was then decided to operate with 1.5% hydrogen in the CO_2 input. After three days further operation, an increase in leakage of CO_2 into the oxygen envelope required another examination. One drum was found to have deteriorated to the point of substantial porosity on the electrolyte faces. It was snipped out and the manifold tubes were brazed shut, which demonstrates the versatility of the manifold-multi-cell arrangement. Four days further operation were obtained with oxygen yield greater than 90% of theoretical, when an open circuit appeared due to grid-electrolyte detachment. At this time the CO_2 leakage into the oxygen stream was up to 4%. The electrolyte disks had deteriorated to the point where their useful life was at an end and the test was terminated. This electrolyzer performed satisfactorily for 101 days producing 24 amperes equivalent of breathable oxygen at 100% faradaic efficiency and functioned for 14 days additionally at a less reliable level.

5.4 ONE-DRUM UNIT Z-19

This unit was constructed to determine the reliability and operating characteristics of a grid design intended to improve current distribution over the cell faces (style K-1E). Expanded platinum mesh with 0.5 mm (0.020 inch) peripheral platinum wire rim was fired to the electrolyte faces with platinum paste as in previous electrodes. Current density concentration was changed by tapping the peripheral rim at four points with 0.5 mm platinum lead wires which were looped away from the electrode to a welded connection with a 1 mm gold alloy wire main lead. The gold alloy wires then were sealed through the drum walls, for inside cell faces, or carried around the drum, for outside cell faces, and connected in series as in previous units.

The 1 cm high drum body was made of calcia-stabilized zirconia and the electrolyte disks were of $(ZrO_2)_{0.93}(Sc_2O_3)_{0.07}$. The drum was brazed to platinum alloy tubes, the entrance tube having the two-port nozzle previously reported. Alumina manifold tubes supported the drum in a mullite envelope for operation in a horizontal furnace.

Operation was started on CO_2 electrolysis, omitting the customary oxygen pre-treatment to determine the effect on electrode adherence. Immediately on reaching the operating temperature of 875°C, a current of 2 A per cell (100 mA/cm^2) was applied. The oxygen yield was 100% of theoretical and the CO_2 leakage remained nearly constant at 0.32%. After 161 hours, the current was reduced to make current-voltage measurements. The relationship was linear up to the chosen limit of 2 A and the cells showed slightly less resistance than those of one-drum electrolyzer Z-8 (Ref. 2). Operation continued at 2 A until, on the 42nd day, one cell shorted out. A somewhat downward trend in oxygen yield appeared after the 35th day, as shown in the operating data plot, Fig. 5-6.

The drum was opened and the short was found to be due to sagging of a gold lead wire. No deterioration of electrolyte or grids appeared.

5.5 TWO-DRUM UNIT Z-20

Special drum bodies with length twice that of the standard drum were prepared (21 mm vs. 10.5 mm) to test the effect of

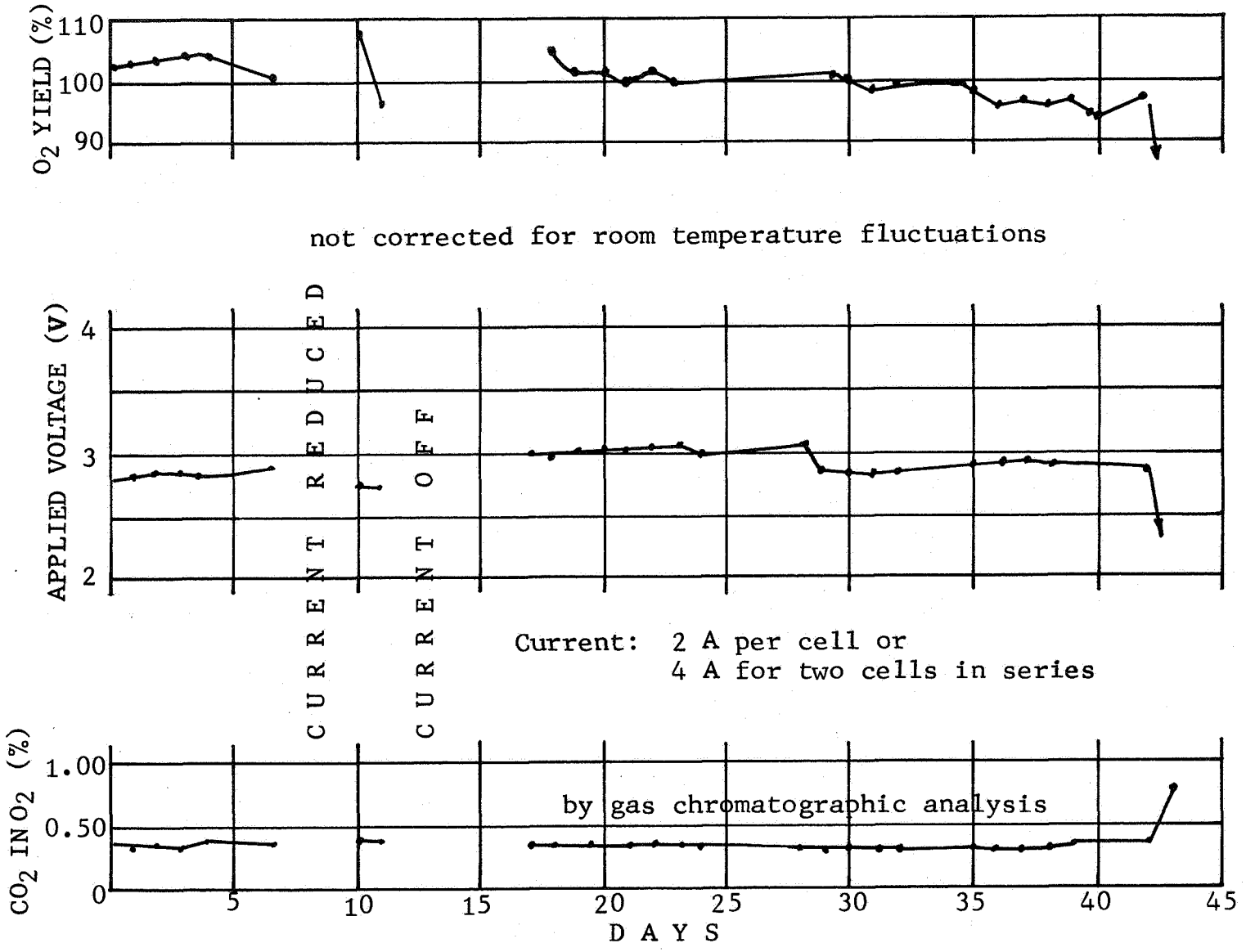

Fig. 5-6 Performance of Two-Cell Electrolyzer Z-19
Operating at 100 mA/cm^2 and 875°C

reducing leakage current paths which have been postulated as a possible source of drum failure. Stabilized zirconia as used for the drum bodies is about 20 times less conductive than the electrolyte zirconia; however, it can carry some current and there was evidence of some electrolytic degradation on some fracture faces on failed parts in the six-drum modules of the one-man unit (Z-10, Z-11, and Z-12). Current leads passing through the drum wall of unit Z-20 were located asymmetrically such that the path through the wall from each lead to the electrode to which it was connected was 2.0 mm and the path to the inner electrode of the other disk which was at a different potential, was 12.0 mm.

The electrolyte material in this unit was $(ZrO_2)_{0.93}(Sc_2O_3)_{0.08}$. Grids were style K-9 described above in Section 4. The central tap (K-9, side A) was located inside the drum for both cells; thus, the four cells of two drums could be conveniently connected in series. The current path through the electrolyte, from the peripheral tap on one side of the cell to the central tap on the opposite side, was intended to allow high current density (to 200 mA/cm^2) without the "hot-spot" electrolyte degradation which appeared with some previous designs. One drum, F-227, used gold paste for the electrode. Hydrogen was added to the gas stream so that the hydrogen content would be greater than that obtained solely by water saturation. This addition made a total of 13% $\pm$ 3% H_2 during this operation. Operating data are shown in Fig. 5-7. There was a considerable instability, with recurring peaks of increased resistance (high applied voltage) corresponding with lows in oxygen yield. The individual cell voltages showed the high resistance to be in drum F-227, which had the gold paste electrode. Operation continued until the 43rd day (1032 hours), when a power failure shut down the unit. On re-starting, extreme high resistance and a severe jump in CO_2 level indicated major damage had occurred. The unit was cooled and dismantled for examination.

Drum F-229 was in good condition. Only a slight discoloration of one outside electrolyte surface appeared, and the grids were still well attached. Drum F-227 had deteriorated badly. The electrolyte surfaces had degraded and the inner grids had detached. A crack across one electrolyte disk was the source of the gas leak which appeared at the re-start attempt.

It is clear that the gold paste electrode is not acceptable. On the other hand, drum F-229, with platinum electrodes, performed very well during this test, and was still usable after greater than 1000 hours of operation.

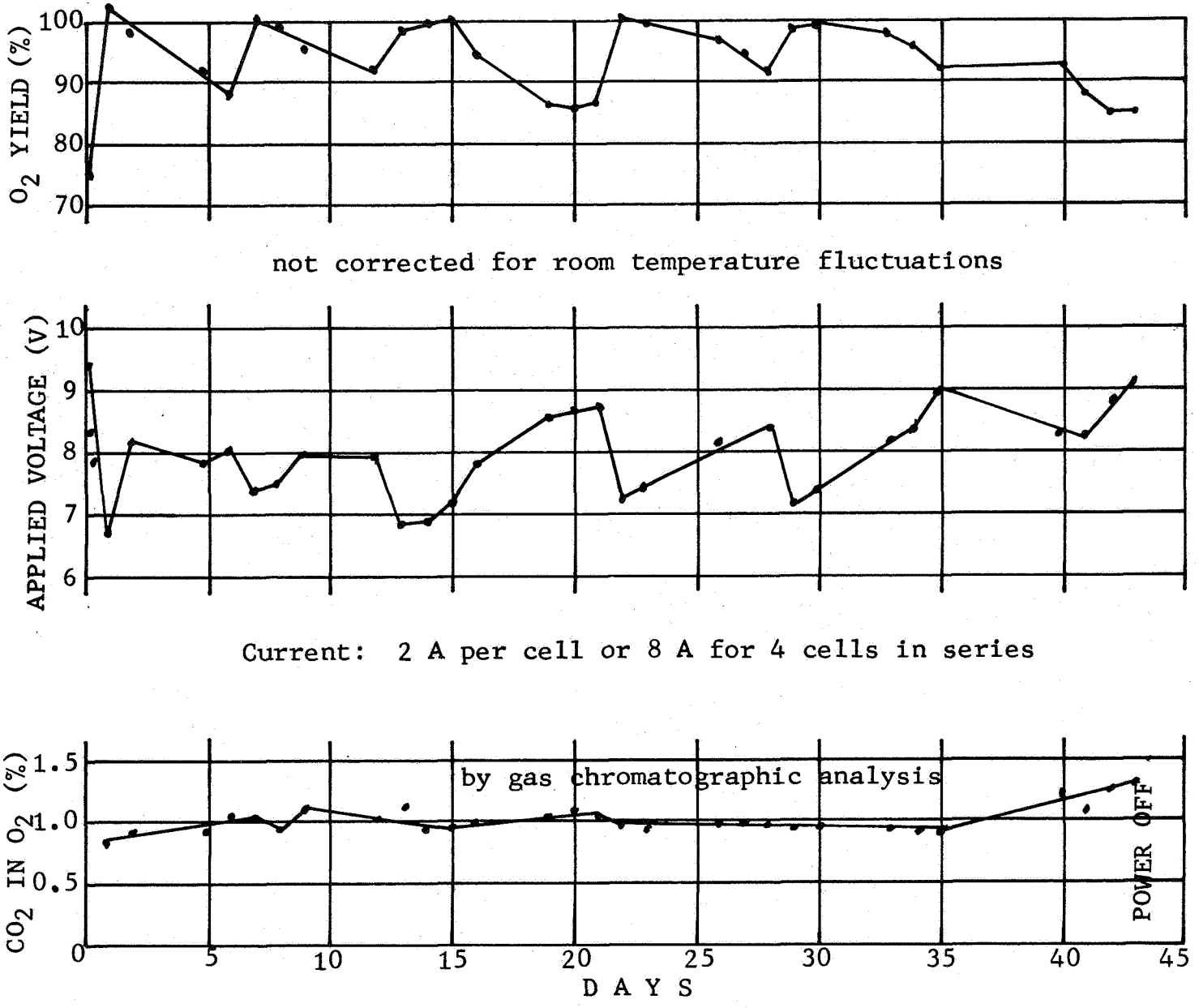

Fig. 5-7 Performance of Four-Cell Electrolyzer Z-20 Operating at 100 mA/cm^2 and 875^{o}C

5.6 ONE-DRUM UNIT Z-21

Unit Z-21 was assembled for electrolysis test as a prototype of the large eight-drum unit Z-24, then in preparation. It was the first test of the heavy gold alloy expanded mesh grid style, discussed in Section 4. In addition, this electrolyzer had an auxiliary electrode in the form of an extra voltage tap wire incorporated into the edge seal braze of the top disk. It was used to measure potential distribution from the rim of the platinum grid to the edge of the electrolyte disk, and from the edge of the electrolyte disk down the drum wall to the radial current lead through the drum wall.

The voltages observed from outer grid to electrolyte edge and from electrolyte edge to current lead (inner grid) always added up to the total voltage measured from outer grid to inner grid.

The unit was placed into a horizontal furnace and taken to operating temperature (~870°C). It was pre-treated by electrolyzing oxygen from drum to envelope and from envelope to drum at currents from 0.5 to 3 A for a period of four days. It was then placed in operation electrolyzing CO_2 at 870°C. Hydrogen was added to reach a 15% H_2 level in the gas inlet stream.

Operating results are summarized in Fig. 5-8. A power failure occasioned shutting down the unit after 15 days. When it was re-started, there was no change in the average oxygen yield and CO_2 level in the oxygen. Operation then continued until a drastic rise in CO_2 content of the oxygen stream indicated a leak on the 63rd day. Oxygen yield had begun to decline at the 58th day, suggesting incipient failure.

When the abrupt CO_2 leakage appeared, the unit was shut down and dismantled. Degradation of the electrolyte was severe and both disks had cracked. The inner grids had detached from the electrolyte surfaces. Satisfactory operation for 1390 hours suggests that the deterioration appeared subsequent to that time and only progressed rapidly during the remaining two days operation. The behavior of this electrode-grid style was discussed in Section 4.

Operating data for unit Z-21 are given in Table 5-3. The extent of conversion of CO_2 to CO was increased during the run, by reducing the CO_2 influx rate, until it reached 82.5%. At

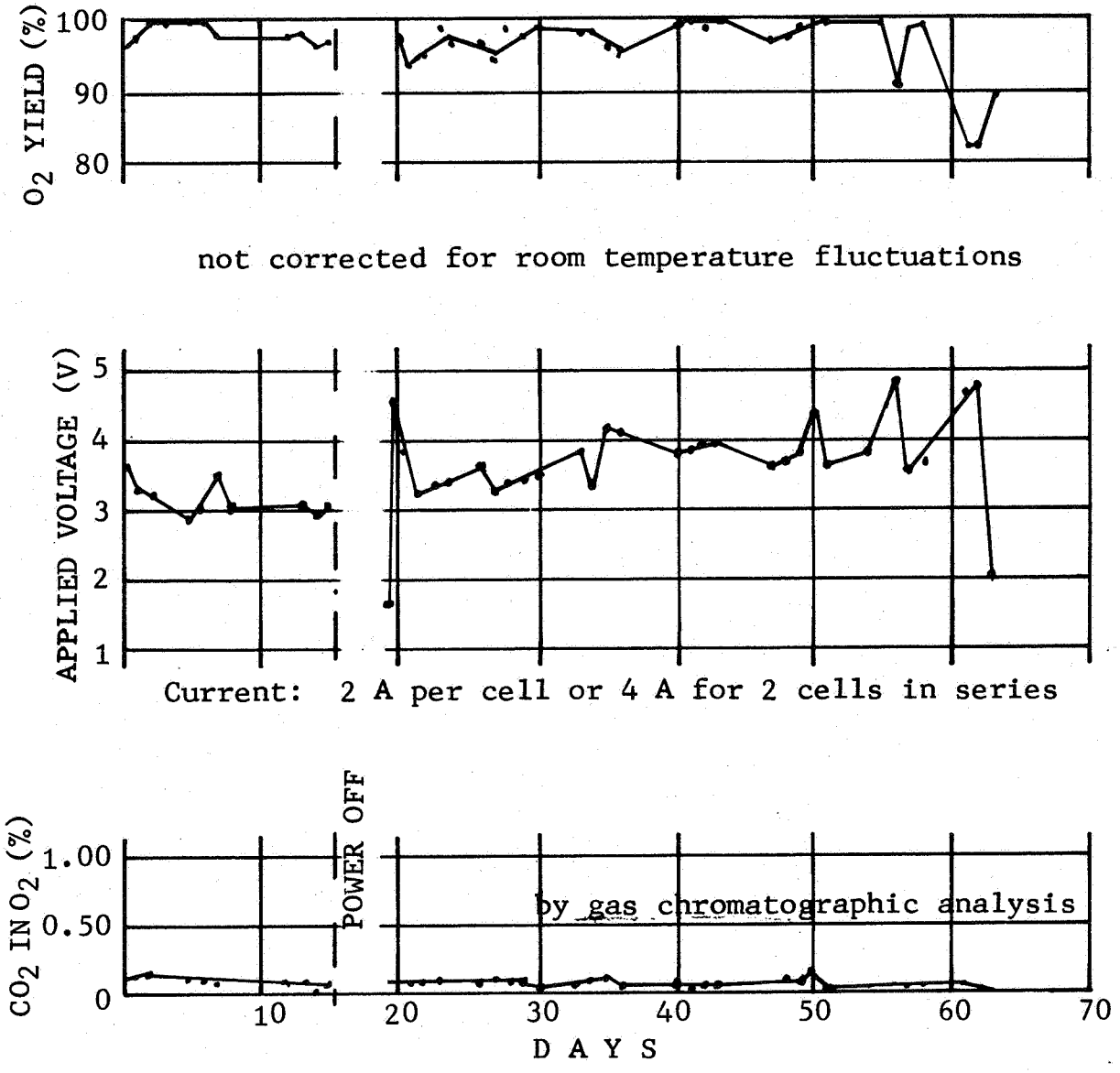

Fig. 5-8 Performance of Two-Cell Electrolyzer Z-21 Operating at 100 mA/cm^2 and 870°C

Table 5-3

OPERATING DATA FOR UNIT Z-21

Day	Cell Voltages (V)		O_2 Yield (%)	CO_2 in O_2 (%)	CO in CO_2 (%)
1	1.92	1.77	96	-	-
1	1.53	1.79	100.5	-	-
2	1.46	1.79	98	0.14	26.5
3	1.47	1.81	100	0.15	26.0
6	1.41	1.43	100	0.12	27.1
7	1.46	1.47	100	0.12	27.6
8	1.65	1.88	98	0.10	34.6
13	1.50	1.49	98	0.10	41.8
14	1.54	1.53	98	0.10	41.5
15	1.47	1.44	96.5	0.03	47.0
16	1.52	1.48	97	0.08	46.7
16	Power failure				
16	Power up				
19	2.31	2.30	-	-	-
20	1.94	1.92	98.4	0.12	46.2
21	1.61	1.59	94	0.11	46.0
22	1.68	1.65	95	0.11	47.0
23	1.72	1.67	99	0.10	46.1
26	1.91	1.72	96.5	0.10	46.2
27	1.64	1.63	94	0.10	49.0
28	1.67	1.67	98.6	0.10	47.8
29	1.70	1.72	98	0.10	47.3
30	1.75	1.72	99	0.07	47.9
33	2.05	1.80	98	0.08	45.8
34	1.65	1.67	98	0.10	47.2
35	2.15	2.02	96	0.13	49.0
36	2.10	1.95	95.4	0.07	47.4
40	2.00	1.76	99.5	0.07	48.3
41	2.03	1.80	100	0.05	45.9
42	2.07	1.82	99	0.07	49.9
43	2.08	1.83	100	0.06	48.1
47	1.75	1.86	97	0.03	52.3
48	1.80	1.89	97	0.13	59.4
49	1.85	1.90	99	0.06	59.3
50	2.20	2.37	97	0.11	57.5
51	1.80	1.80	100	0.04	61.1
54	1.96	1.86	100	0.08	60.0
55	2.04	1.89	100	0.05	59.1
56	2.46	2.42	90	0.07	53.6
57	1.71	1.82	99	0.07	59.8
58	1.75	1.86	100	0.08	60.7
59	-	-	-	-	82.5
62	2.48	2.35	82	0.06	70.0
63	2.48	2.37	81.5	0.04	69.5
64	0.76	0.02	89	3.87	21.6
65	Electrolysis Terminated				

this point, the faradaic current efficiency declined significantly below 100% and failure of the unit occurred shortly afterward. The power failure on day 16 caused an interruption of operation of 22 hours. The CO_2 feed gas stream into the electrolyzer contained 15% hydrogen from the start of the run through the 47th day, 18% hydrogen from the 48th though the 58th day, and 24% hydrogen from the 59th day to the end of the run. The current was maintained at 2 A per cell throughout the run until day 64 when degradation of one cell required termination of the test.

5.7 ONE-DRUM UNIT Z-23

Unit Z-23 consists of one drum with each cell having grid style K-19 (see Section 4, above). This unit has been provided with current carrying extension leads from each cell out to the control panel of the electrolysis test stand. The wiring style and control mode (voltage or current control) can then be selected or changed at any time. Both cells were connected in parallel on the control panel, with an ammeter on the lead to each cell, for operation at constant voltage from a single power supply. Electrolysis of dry CO_2 containing 19 $\pm$ 4% hydrogen was started, without oxygen electrolysis pre-conditioning, using a constant voltage of 2.00 $\pm$ 0.06 V across each cell.

Operating data, to date, are shown in Table 5-4 and in Fig. 5-9. Oxygen yield has continued at 100% of theoretical throughout this run, and the CO_2 leakage into the oxygen has remained substantially below 0.5%. A generally increasing trend in resistance (reduced current) occurred from the 7th to the 48th day of operation. The applied voltage was increased to 2.20 V on day 49 to bring the average current per cell back to 2 A. Conversion per pass of CO_2 to CO ranged from 29 to 92%, because of experimental changes in the inlet CO_2 rate, with conversion above 75% during most of the run. Operation continues at a CO content in the effluent CO-CO_2 stream from the cathode chambers of ~80%.

5.8 EIGHT-DRUM UNIT Z-24

This is the largest module, in terms of number of drums, that has been assembled. It consists of eight drums (16 cells, total electrode area 320 cm^2). The grids on all of the cells

Table 5-4

OPERATING DATA FOR UNIT Z-23

Day	Voltage of Each Cell	Current (A)		O_2 Yield (%)	CO_2 in O_2 (%)	CO in CO_2 (%)
1	2.00	2.10	2.12	101.5	-	-
2	1.98	2.15	2.65	100	0.04	55.7
5	1.98	2.49	2.92	100	0.09	59.8
5	2.01	2.43	2.41	103	-	88.0
6	2.02	2.56	2.37	100.1	0.14	92.3
6	2.02	2.54	2.36	103	-	92.8
7	1.99	2.82	2.58	101	0.07	82.8
8	1.99	2.76	2.52	105	0.12	82.9
9	2.01	2.67	2.43	102	0.16	79.1
12	2.05	2.63	1.89	101	0.17	73.0
13	2.04	2.79	1.89	99	0.16	71.5
13	2.03	2.89	1.92	103	0.29	54.0
14	2.04	2.84	1.88	103	0.35	51.9
15	2.04	2.86	1.86	101	0.46	-
15	2.04	2.79	1.83	100	-	52.4
16	2.05	2.56	1.79	103	0.42	54.0
19	2.04	2.77	1.80	102.5	0.33	55.7
20	2.04	2.72	1.75	101	0.32	55.1
21	2.05	2.54	1.75	102	0.31	53.6
21		Electrolysis off				
22	2.06	2.32	1.84	101	0.33	51.5
23	2.02	2.26	1.60	100	0.25	61.0
26	2.02	2.24	1.65	101.5	0.25	76.0
27	2.02	2.25	1.66	99.8	0.27	75.8
28	2.02	2.21	1.65	103	0.29	75.8
29	2.03	2.18	1.64	102	0.31	75.4
34	2.04	2.04	1.58	101	0.31	71.5
35	2.04	1.98	1.58	102	0.27	73.4
36	2.04	1.99	1.59	100	0.23	73.0
37	2.03	2.08	1.68	103	0.22	76.8
40	2.03	2.00	1.70	102	0.25	74.7
41	2.03	1.99	1.70	100	0.20	76.4
42	2.01	1.96	1.68	104	0.18	76.4
43	2.00	1.93	1.67	104	0.18	76.0
44	2.00	1.91	1.66	100	0.18	74.0
47	2.01	1.88	1.64	101	0.17	74.2
48	2.00	1.88	1.66	100	0.16	73.5
49	2.20	2.18	2.02	100	0.15	76.0
50	2.20	2.16	1.96	101	0.14	74.0
51	2.18	2.42	2.01	101	0.14	80.0
54	2.19	2.29	1.93	99	0.14	77.2
55	2.20	2.27	1.92	97	0.13	82.8
56	2.20	2.21	1.90	100	0.15	80.5
57	2.20	2.17	1.88	101	0.16	80.0
58	2.20	2.13	1.84	103	0.27	83.5
61	2.20	2.11	1.78	100	0.16	77.3
		Electrolysis Continuing				

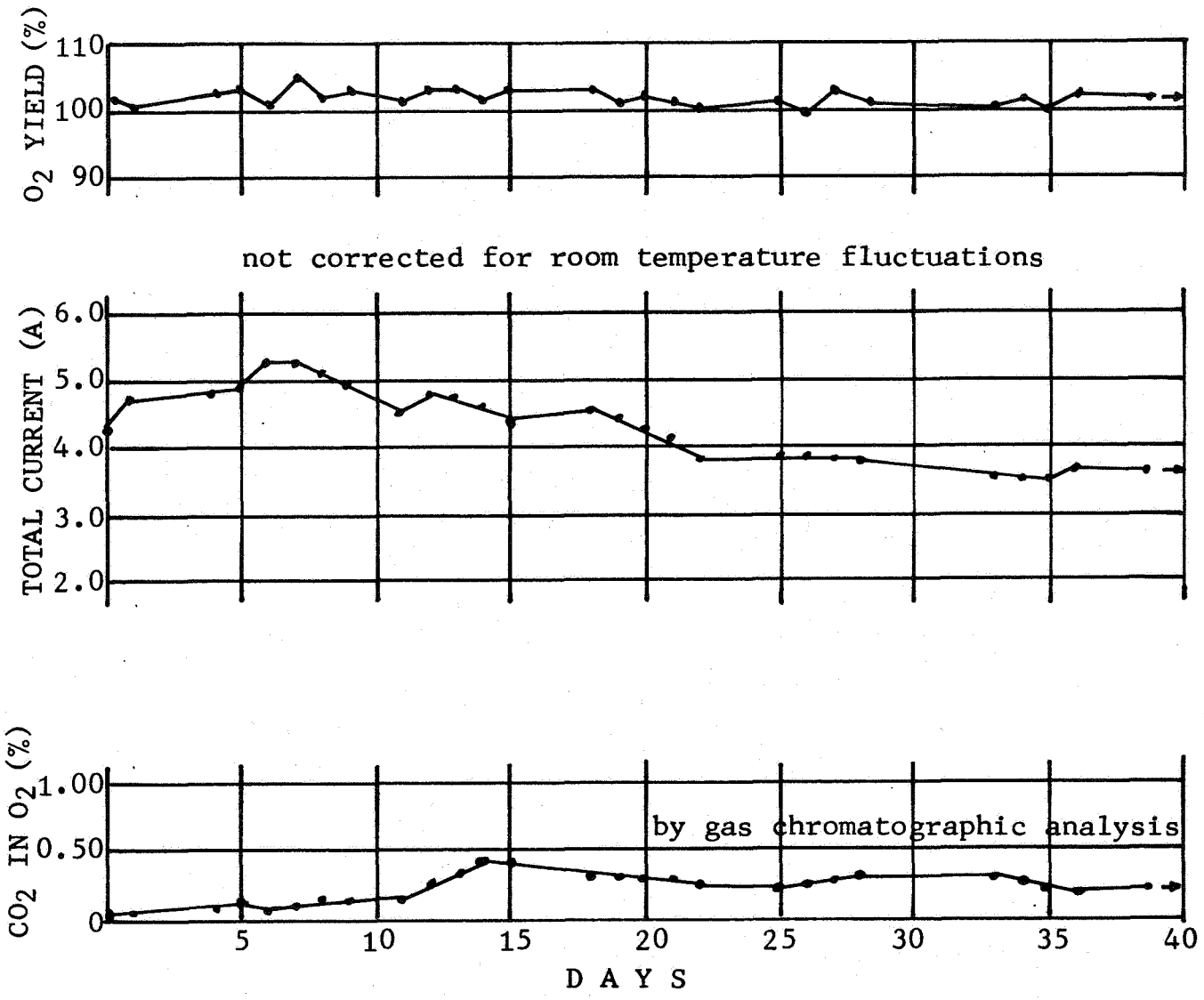

Fig. 5-9 Performance of Two-Cell Electrolyzer Z-23
Operating at Constant Voltage and 870°C

are heavy expanded gold alloy, some of which have been furnace spot brazed to the platinum plate on the disk (see Section 4). One cell contains an auxiliary electrode consisting of an electrical lead spot brazed to a small, electrically isolated, plated area on the inside of the top disk near the edge. A gas port tube has been used as a path for bringing the auxiliary electrode signal through the drum body. This unit has been assembled to demonstrate the feasibility of construction of large multi-drum modules by the present fabrication technique. Life testing on CO_2 electrolysis is being carried out under conditions more severe than those used for the previous life-tested multi-drum unit, Z-17. The degree of conversion per pass is greater, and the special low drum body voltage brought about by the double series wiring of unit Z-17 has been eliminated. This electrolyzer constitutes a one-fourth man unit (32 A) at the present operating level of 100 mA/cm^2.

Operation was started directly on CO_2 electrolysis without oxygen pre-treatment. Hydrogen was added to the gas for a 15% total hydrogen content. Operating data are shown in Table 5-5 and Fig. 5-10. The CO_2 concentration in the O_2 output leveled off at about 0.7% after the first 10 days. It appears that a minor leak developed in that period, but the leak rate did not increase further. Oxygen yield remains steady at nearly 100% of theoretical through the present date. The degree of conversion per pass of CO_2 to CO was in the range 51 to 54% for the first 26 days. On the 27th day the flow rate of CO_2 was decreased slightly to increase the CO concentration in the cathode effluent gas. This increase in conversion per pass had no other apparent effect on the operation of the electrolyzer.

A steady, slightly increasing trend in resistance (increase in applied voltage) is apparent (Fig. 5-10) for the first 42 days. At that point it was necessary to shut down briefly and purge the hydrogen inlet lines in order to change hydrogen supply bottles without hazard of explosion. On restarting, resistance increase of about 10% across the electrolyzer appeared. Individual cell voltages indicated that approximately equal portions of the change occurred in every cell; hence, the effect was general rather than some localized failure. Individual cell voltage data are given in Table 5-6 at seven day intervals.

Table 5-5

OPERATING DATA FOR UNIT Z-24

Day	O_2 Yield (%)	CO_2 in O_2 (%)	CO in CO_2 (%)
1	98.4	0.37	53.4
5	99	0.18	53.2
6	98	0.53	53.1
7	99	0.41	53.8
8	100	0.58	52.7
12	99	0.68	52.7
13	99	0.63	53.2
14	97	0.69	52.5
15	100	0.78	53.2
16	100	0.72	53.4
19	99	0.81	51.2
20	99	0.75	52.8
21	98	0.73	53.5
22	99	0.79	53.1
23	98	0.77	53.5
26	98	0.87	53.5
27	98	0.73	58.5
28	98	0.68	58.3
29	96	0.80	58.4
30	99	0.72	59.5
33	96.5	0.67	58.5
34	96.5	0.71	59.3
35	99	0.74	59.0
36	96.5	0.70	59.0
37	98	0.74	58.7
40	100	0.78	59.5
41	99	0.76	59.4
42	96.5	0.69	59.3
43	100	0.79	59.7
44	97	0.68	62.7
47	97	0.69	59.2
48	98	0.74	58.7
49	99	0.72	58.9
50	99	0.78	59.2
55	100	0.69	59.8
56	100	0.67	60.1
57	97	0.64	59.2
58	98	0.65	58.9
61	99	0.66	59.4
62	99	0.70	59.3
63	98	0.71	59.2
64	98	0.69	58.8
65	98	0.71	58.8
68	98.5	0.71	59.0
69	97	0.73	59.7
70	97	1.14	59.8
71	98	0.64	59.3
72	98	0.80	59.6
75	99	0.80	60.2
76	97	0.33	58.9
77	98	0.72	59.9
78	99	0.67	60.2
79	100	0.78	61.0
82	98	0.72	59.5
Electrolysis Continuing			

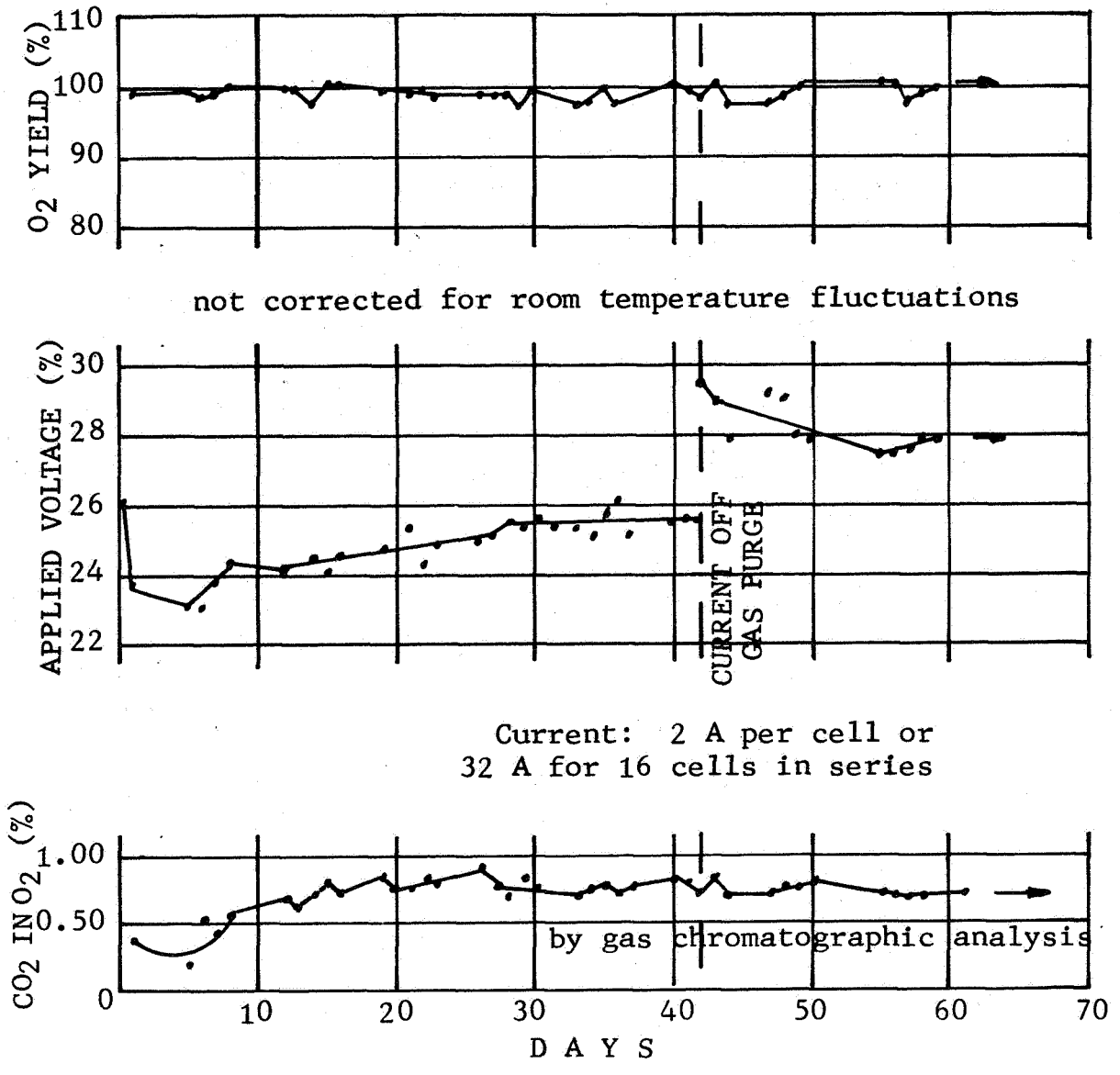

Fig. 5-10 Performance of Sixteen-Cell Electrolyzer Z-24 Operating at 100 mA/cm^2 and 870°C

Table 5-6

CELL VOLTAGES FOR UNIT Z-24

Day	CELL NUMBERS *											
	1 & 2	3	4	5	6	7 & 8	10	11	12	13 & 14	15	16
1	3.48	1.71	1.69	1.31	1.34	2.70	1.35	1.29	1.32	3.04	1.67	1.90
8	3.15	1.48	1.47	1.40	1.41	3.26	1.64	1.73	1.55	2.85	1.41	1.59
15	3.16	1.50	1.51	1.42	1.41	2.94	1.74	1.47	1.52	2.83	1.46	1.64
22	3.14	1.46	1.46	1.46	1.45	3.02	1.79	1.38	1.45	2.91	1.49	1.65
29	3.19	1.47	1.52	1.47	1.45	2.98	1.84	1.45	1.50	3.43	1.57	1.76
36	3.26	1.52	1.53	1.53	1.52	3.02	1.82	1.55	1.58	3.03	1.89	2.18
43	3.46	1.62	1.67	1.68	1.66	3.33	1.99	1.70	1.74	3.54	1.77	1.96
50	3.66	1.55	1.58	1.73	1.69	3.64	1.80	1.68	1.75	3.17	1.78	2.00
57	3.36	1.56	1.60	1.56	1.58	4.00	1.89	1.63	1.67	3.36	1.65	1.86
64	3.45	1.53	1.60	1.63	1.72	4.25	1.88	1.62	1.71	3.28	1.85	2.14
71	3.38	1.56	1.65	1.83	1.82	4.45	1.91	1.85	1.97	3.30	1.66	1.90
78	3.31	1.62	1.72	1.98	2.00	3.85	1.83	1.93	2.00	3.30	1.66	1.91

*No voltage data were taken for cell no. 9 because of control panel limitations

As discussed above, electrolyzer Z-24 has operated on life test for nearly three months producing breathable oxygen from CO_2. Electrolyzer Z-24 continues in operation at 870°C, ~100% oxygen yield, 0.7% CO_2 in the oxygen, 60% conversion per pass, and relatively constant applied voltage at 2 A per cell or a total current of 32 A.

Section 6

DISCUSSION

Each of the eight electrolysis modules constructed and operated during the nine-month contract period covered by this report electrolyzed carbon dioxide to produce oxygen containing less than 1% total impurities (as determined by gas chromatography). This performance indicates that the basic design principles that have guided this work remain valid. The evolutionary changes that were made in design detail, materials, and fabrication methods were beneficial and led to this improved performance. Reliable long-term operation with a breathable oxygen output not significantly contaminated by CO_2 is essential if this system is to be used for aerospace life support without being burdened by the large power penalty that is imposed by CO_2 scrubbing (Ref. 9). Production of breathable oxygen (arbitrarily taken as O_2 purity of >99%) by these modules for periods as long as 101 days shows that the major problems of solid oxide electrolyzer technology have been solved, and that integration of a one-man electrolyzer with a CO disproportionator and closed recycle loop is the logical next step.

Operating data for the electrolyzers for the time period when each one was producing oxygen of >99% purity from CO_2 are summarized in Table 6-1. In some cases these data represent the total period of the test, but in most cases the units were run further to where CO_2 leakage had gone above 1% or electrical anomalies had occurred. Complete test data for each of these units were given in Section 5, above. Each electrolyzer was fabricated for a particular purpose during the evolution of the technology, as discussed above in Sections 3, 4, and 5. The most interesting are units Z-17 and Z-24 because of their large size and long periods of successful operation.

Unit Z-17 constitutes a 1/5 man module at the current density (100 mA/cm^2) at which it was operated. Operation at this current density was continuous for the 101-day period except for an interruption on the 86th day shown in Table 5-1 and discussed in sub-section 5.3. No maintenance or repair work was performed on this, or any other, unit during the operating periods shown in Table 6-1. Production of oxygen containing 0.11 to 0.49% CO_2 at 100% faradaic efficiency for 101 days

Table 6-1

SUMMARY OF ELECTROLYZER OPERATION FOR PRODUCTION OF OXYGEN OF >99% PURITY*

Module Number	Number of Cells	Electrode Area (cm^2)	Total Current (A)	Average Cell Voltage (V)	CO_2 in O_2 (%)	Conversion Per Pass (%)	Operating Period at >99% O_2 Purity (Days)
Z-13	4	80	16	2.4	0.10 to 0.33	28.1 to 38.6	12
Z-14	4	80	16	2.7	0.07 to 0.85	29.5 to 34.8	11
Z-17	12	240	24	1.8	0.11 to 0.49	20.1 to 27.0	101
Z-19	2	40	4	1.4	0.26 to 0.38	17.6 to 48.7	42
Z-20	4	80	8	2.0	0.82 to 0.94	23.7 to 50.0	41
Z-21	2	40	4	1.7	0.03 to 0.15	26.0 to 60.7	58
Z-23	2	40	4	1.7	0.04 to 0.46	51.5 to 92.8	61 (continuing)
Z-24	16	320	32	1.6	0.18 to 0.87	51.2 to 62.7	82 (continuing)

*The operating temperature of each module was ~870°C. In each case, average current efficiency was ~100% during the period of operation at <1% CO_2 in the O_2.

demonstrates the significant progress that has been achieved since the test of the one-man unit discussed in Ref. 2 and in sub-section 5.1, above.

Units Z-19, Z-20, Z-21, and Z-23 were each fabricated to aid in improving the various aspects of design and fabrication that were discussed in Sections 3, 4, and 5. As a result of test data from these units, unit Z-24 was constructed. This 16-cell, 32-A, 1/4 man unit has run for 82 days and continues to operate, producing breathable oxygen at 100% faradaic efficiency.

The significant aspects of each of these electrolyzers are as follows:

Unit Z-13	new electrodes and grids, new gas port entry tubing, high-conductivity electrical leads, and assembly by torch brazing
Unit Z-14	parallel electrical connections for the two cells of each drum
Unit Z-17	new gas port entry nozzle, horizontal configuration in furnace, two sets of cells wired in series independently of each other, new electrodes and grids
Unit Z-19	new electrodes and grids
Unit Z-20	larger drum bodies, gold paste electrodes on one drum (showed gold paste electrodes perform very poorly compared to platinum)
Unit Z-21	one drum prototype of eight drum unit Z-24, new electrodes and grids, operated at high conversion per pass
Unit Z-23	parallel electrical connections, constant voltage operation, high conversion per pass
Unit Z-24	eight-drum unit incorporating the best features of all prior units

The progress represented by these electrolyzers, and by the other work of this contract period, can be evaluated with reference to the recommendations for future work made one year ago in the Second Annual Report (Ref. 2, pp. 93 and 94). This evaluation is as follows:

1) Work on electrodes and grids has resulted in marked improvements. Further experiments of the same type should lead to even better electrodes and grids, to longer operating times for >99% oxygen, and higher current densities.

2) Electrical leads of higher electrical conductivity have been adopted as standard (Au, 5% Pd).

3) The gas entry nozzles have greatly improved the flow pattern, and the present degree of mixing appears to be adequate.

4) Better control of hot-pressing parameters has eliminated the problem of electrolyte disk porosity.

5) Other electrolyte compositions proved to be inferior to scandia-stabilized zirconia. Therefore, scandia-stabilized zirconia has been adopted as standard.

6) Experiments with cells larger than 20 cm^2 were not conducted, but the idea remains appealing.

7) Experiments to date with drum bodies other than zirconia have been unsuccessful, but work should continue to find either non-zirconia body material or zirconia with more controllable and predictable properties than is the case at present.

8) Torch brazing the drums to the gas manifolds has been adopted as a standard assembly procedure.

9) Better packaging is contemplated as a part of the work of the next contract period.

10) A considerable amount of operating data has been obtained for the production of breathable oxygen and more data are being obtained from CO_2 electrolysis modules presently continuing in operation.

11) Some work was done to improve the canister catalytic reactor (sub-section 3.7, above) and additional work is required.

Section 7

REFERENCES

1. J. Weissbart et al., "Development of a CO_2-H_2O Solid Oxide Electrolyte Electrolysis System," First Annual Report, Contract NAS2-4843, Applied Electrochemistry Incorporated, Mountain View, California, May, 1969

2. J. Weissbart and W. H. Smart, "Development of a CO_2-H_2O Solid Oxide Electrolyte Electrolysis System," Second Annual Report, Contract NAS2-4843, Applied Electrochemistry Incorporated, Mountain View, California, May, 1970

3. J. Weissbart, W. H. Smart, and T. Wydeven, "Oxygen Reclamation Using a Solid Oxide Electrolyte," Aerospace Medicine, 40, 136 (1969)

4. J. H. Perry, Chemical Engineers' Handbook, 4th Edition, McGraw-Hill, 1963, pp. 6-31

5. T. F. Berry, R. N. Ames, and R. B. Snow, J. Am. Chem. Soc., 39, 308 (1956)

6. P. L. Walker, Jr., J. F. Rakszawski, and G. R. Imperial, J. Phys. Chem., 63, 133 (1959)

7. P. L. Walker, Jr., J. F. Rakszawski, and G. R. Imperial, J. Phys. Chem., 63, 140 (1959)

8. J. Weissbart and W. H. Smart, "Study of Electrolytic Dissociation of CO_2-H_2O Using a Solid Oxide Electrolyte," First Annual Report, Contract NAS2-2810, Lockheed Missiles and Space Co., Palo Alto, California, NASA Contractor Report CR-680, February, 1967

9. "Trade-off Study and Conceptual Designs of Regenerative Advanced Integrated Life Support Systems (AILSS)," Contract NAS1-7905, Hamilton Standard Division of United Aircraft Corporation, Windsor Locks, Connecticut, NASA CR-1458, January, 1970